NEUROSCIENCE

TDP-43 impairs sleep in *Drosophila* through *Ataxin-2*–dependent metabolic disturbance

Alexandra E. Perlegos[1,2]†, Jaclyn Durkin[3,4]†, Samuel J. Belfer[1,3]†, Anyara Rodriguez[3], Oksana Shcherbakova[2], Kristen Park[1], Jenny Luong[3], Nancy M. Bonini[1,2,5]*, Matthew S. Kayser[3,5,6]*

Neurodegenerative diseases such as amyotrophic lateral sclerosis and frontotemporal dementia are associated with substantial sleep disruption, which may accelerate cognitive decline and brain degeneration. Here, we define a role for trans-activation response element (TAR) DNA binding protein 43 (TDP-43), a protein associated with human neurodegenerative disease, in regulating sleep using *Drosophila*. Expression of TDP-43 severely disrupts sleep, and the sleep deficit is rescued by *Atx2* knockdown. Brain RNA sequencing revealed that *Atx2* RNA interference regulates transcripts enriched for small-molecule metabolic signaling in TDP-43 brains. Focusing on these *Atx2*-regulated genes, we identified suppressors of the TDP-43 sleep phenotype enriched for metabolism pathways. Knockdown of *Atx2* or treatment with rapamycin attenuated the sleep phenotype and mitigated the disruption of small-molecule glycogen metabolism caused by TDP-43. Our findings provide a connection between toxicity of TDP-43 and sleep disturbances and highlight key aspects of metabolism that interplay with TDP-43 toxicity upon *Atx2* rescue.

INTRODUCTION

The rate of neurodegenerative disease diagnoses is steadily increasing with an aging population (*1*, *2*). In addition to prominent cognitive symptoms, sleep disturbances are a large contributor to the decreased quality of life of patients and caregivers (*3*, *4*). Recent work suggests a bidirectional relationship between sleep and Alzheimer's disease pathology: abnormal accumulation of the pathogenic proteins tau and amyloid-β (Aβ) worsen sleep, while inadequate sleep accelerates the buildup of tau and Aβ (*5*–*10*). Because of the close relationship between sleep features and dementia, serial cognitive testing is common in the workup of parasomnias and can be helpful for early diagnosis of neurodegenerative diseases (*11*, *12*). Sleep disturbances are also beginning to be recognized in the disease course of amyotrophic lateral sclerosis and frontotemporal dementia (ALS/FTD). Long considered a disease that solely affected motor neurons, recent work has linked cognitive and autonomic dysfunction to ALS/FTD disease progression (*13*). Findings indicate that sleep is notably disrupted in patients with ALS/FTD (*14*, *15*); therefore, elucidating cellular mechanisms that couple neurodegenerative diseases to sleep disruption could reveal additional treatment avenues.

Neurodegenerative diseases are characterized by the aberrant accumulation of key proteins that induce toxicity to the brain. Models of neurodegeneration for Alzheimer's disease, ALS, and other diseases have been established in *Drosophila* by directed expression of the human proteins in the fly, followed by characterization of degenerative effects on lifespan, motor function, brain integrity, and other behavioral and anatomical features that reflect the human disease (*16*–*18*). The genetic tractability of *Drosophila* has enabled large-scale screens to identify modifiers of the human protein toxicity and associated degeneration (*16*, *17*, *19*–*25*). The robust sleep behavior of flies also makes them an excellent system to explore the concurrent relationship between sleep and neurodegenerative disease (*26*–*28*). Previous work has identified sleep deficits in *Drosophila* models of Alzheimer's disease (*27*, *29*), tauopathy (*30*), ALS/FTD (*31*), and Parkinson's disease (*32*, *33*), among others. Several groups have demonstrated that improving sleep by pharmacotherapy (*29*) or behavioral sleep therapy adapted from human techniques (*34*) has positive outcomes in fly models of human neurodegenerative disease, including improved memory performance and extended lifespan.

TAR DNA binding protein 43 (TDP-43) is the protein that accumulates abnormally in nearly all cases of ALS; abnormal TDP-43 inclusions have also been implicated in neurodegenerative diseases including frontotemporal lobar degeneration, primary lateral sclerosis, and progressive muscular atrophy (*35*–*37*). In addition, TDP-43 pathology has been detected in up to ~60% of Alzheimer's cases where it is associated with worse brain atrophy and memory loss (*38*–*42*). Pathological TDP-43 inclusions and consequent neuronal death are thought to be due to a combination of both toxic gain of function and loss of function associated with depletion of TDP-43 from the nucleus and abnormal accumulation of the protein in the cytoplasm (*43*, *44*). Although rare mutations in TDP-43 have been described in ALS and FTD, most disease is associated with the abnormal accumulation of the normal protein (*45*). TDP-43 is a nucleic acid binding protein that plays a critical role in many cellular processes. During periods of stress (heat shock, oxidative stress, or starvation), TDP-43 can shuttle to the cytoplasm and regulate mRNAs to help promote cell survival (*45*–*49*). In disease, TDP-43 accumulates in the cytoplasm of cells in pathological aggregates that can disrupt normal cellular functions and promote chronic stress (*46*, *47*). Abnormal accumulation of TDP-43 also leads to disruption in metabolic pathways such as glucose, lipid, and mitochondrial metabolism (*31*, *50*–*52*). These metabolic changes further contribute to pathological progression and disrupt energy states needed for normal function and stress resolution in neurons (*50*–*53*).

Here, we used *Drosophila* to assess sleep in protein expression models of human neurodegenerative disease. We found that directed expression of TDP-43, which is an established model for ALS/FTD

[1]Neuroscience Graduate Group, Perelman School of Medicine at the University of Pennsylvania, Philadelphia, PA 19104, USA. [2]Department of Biology, University of Pennsylvania, Philadelphia, PA 19104, USA. [3]Department of Psychiatry, Perelman School of Medicine at the University of Pennsylvania, Philadelphia, PA 19104, USA. [4]National Institute of Neurological Disorders & Stroke, National Institutes of Health, Bethesda, MD, 20892, USA. [5]Department of Neuroscience, Perelman School of Medicine at the University of Pennsylvania, Philadelphia, PA 19104, USA. [6]Chronobiology Sleep Institute, Perelman School of Medicine at the University of Pennsylvania, Philadelphia, PA 19104, USA.
*Corresponding author. Email: nbonini@sas.upenn.edu (N.M.B.); kayser@pennmedicine.upenn.edu (M.S.K.)
†These author contributed equally to this work.

(*24*, *47*, *54*–*57*), led to severe sleep deficits. Depletion of *Ataxin-2* (*Atx2*), a modifier of TDP-43 toxicity in flies and mice (*45*, *58*, *59*), reversed the TDP-43 sleep phenotype. We further elucidated the interplay between these proteins using brain RNA sequencing (RNA-seq) analysis to identify transcripts dysregulated by TDP-43 expression that were mitigated by *Atx2* knockdown. On the basis of these RNA-seq findings, a behavioral screen to define additional downstream modifiers of TDP-43 toxicity implicated metabolic pathways through which *Atx2* rescues TDP-43 sleep phenotypes. In TDP-43 flies, metabolic defects and a sensitized sleep phenotype in the setting of starvation raise the possibility that baseline TDP-43–related sleep disruptions reflect a starvation stress. Last, both metabolic defects and the sleep response to starvation were rescued with rapamycin treatment. These findings uncover profound sleep disturbances in this model of neurodegenerative disease and suggest that metabolic dysregulation drives sleep phenotypes of TDP-43 toxicity.

RESULTS

TDP-43 expression impairs sleep in *Drosophila*

To investigate the relationship between neurodegeneration and sleep, we examined sleep in a range of toxic protein expression models of human neurodegenerative disease in *Drosophila*. Expression of these proteins in flies has been shown to recapitulate key aspects of the human diseases, such as neuronal dysfunction and degeneration (*27*, *29*, *60*, *61*); here, we determined whether any of these degeneration models displayed a robust sleep phenotype. To avoid developmental effects and to ensure broad expression of the proteins as in the human disease, we used the hormone-inducible GeneSwitch driver under control of the ubiquitous *daughterless* promoter (*Da*GS). We first assessed sleep during the night after 5 to 7 days of *Da*GS activation on RU486. Most models did not show strong changes in sleep duration or sleep bout characteristics, perhaps due to a later onset of disease pathology (Fig. 1A; fig. S1, A and B; and data S1). These models included expression of human tau (*62*), $A\beta^{Arctic}$ mutant (*63*, *64*), and amyloid precursor protein (APP)/β-site amyloid precursor protein cleaving enzyme (BACE) (*65*) for Alzheimer's disease; the G4C2 repeat expansion and human TDP-43 for ALS/FTD (*22*, *66*); and human α-synuclein for Parkinson's disease (*67*, *68*). We also reduced expression of *Presenilin* of the γ-secretase complex (*69*). Among these models, expression of human TDP-43, associated with sporadic ALS/FTD and found in toxic accumulations in Alzheimer's disease, caused a significant loss of ~200 min of sleep (Fig. 1A) and a nearly threefold reduction in the length of the average sleep bout (fig. S1, A to C).

To confirm these findings, we measured sleep across the day and night in RU486-treated flies compared to vehicle control. A medium-strength expression TDP-43 fly (UAS-*TDP-43*^{37M}; as in Fig. 1A) was assessed, along with an independent insertion with stronger expression (UAS-*TDP-43*^{52S}) (*58*). These lines confer neural degeneration and dysfunction when expressed in the fly eye or nervous system (*24*, *56*, *58*). Both exhibited a marked curtailment of sleep duration during the day and night, along with sleep fragmentation (more short sleep bouts; Fig. 1, B to H). Effects on sleep were not due to the presence of RU486, as flies expressing a control protein yellow fluorescent protein (YFP) had no effect on sleep (fig. S2). We also confirmed the sleep phenotype of *Da*GS>UAS-*TDP-43*^{37M} flies using a higher–spatial resolution multibeam sleep assay (fig. S3, A to D). In both *Drosophila* activity monitoring (DAM) systems (single and multibeam), we detected no locomotor change in TDP-43 flies (fig. S3E), indicating that these animals move normally in the sleep assays. Nonetheless, we considered whether motor neuron toxicity contributes to the sleep changes but found that specific expression of TDP-43 in motor neurons did not recapitulate the observed sleep phenotype (fig. S4); this manipulation resulted in impaired motor function as evidenced by reduced activity (fig. S4, D and H) and an associated increase in measures of sleep (fig. S4, A and E). Together, these results demonstrate a severe sleep phenotype associated with TDP-43 expression that is independent of a role for TDP-43 in motor neuron toxicity.

Next, we examined whether TDP-43 expression impairs sleep homeostasis (sleep rebound following sleep deprivation) or circadian rest:activity rhythms. We found that TDP-43 and YFP control flies responded similarly to mechanical sleep deprivation during the night with near total sleep loss. Despite a reduction in baseline sleep during the day, TDP-43 flies showed normal rebound after sleep deprivation (Fig. 2, A and B), suggesting intact sleep homeostatic functions. TDP-43 expression also had no impact on locomotor rest:activity rhythms under constant conditions (table S1). Thus, TDP-43 does not result in broad sleep/circadian impairments but, instead, specifically disrupts daily sleep duration and continuity. Together, these data indicate that TDP-43 expression causes a robust sleep deficit in flies that is suitable for detailed mechanistic investigation and large-scale screens to define the relationship.

Dose dependence of TDP-43 sleep phenotypes

We considered that there may be a necessary TDP-43 protein "load" that is required to induce sleep loss, below which no sleep phenotypes would be present. To determine whether severity of the sleep phenotype is related to TDP-43 protein level, we titrated the expression of TDP-43 by changing the dosage of RU486. We defined TDP-43 protein levels via Western immunoblot in flies raised on different RU concentrations (Fig. 3A). As expected, TDP-43 protein levels exhibited a dose-dependent relationship to RU486 concentration (Fig. 3B). We then examined sleep in *Da*GS>UAS-*YFP* control and *Da*GS>UAS-*TDP-43*^{52S} flies raised on these same concentrations of RU486 (Fig. 3C). TDP-43 flies showed increasing sleep loss as the dosage of RU486 was increased, suggestive of a direct correlation between protein amount and impact on sleep duration (Fig. 3, D and G). In contrast, sleep continuity appeared more sensitive to TDP-43 levels: even at the lowest dose of RU486, which was associated with relatively modest TDP-43 expression levels, we observed a severe fragmentation of sleep with marked shortening of sleep bout length and increase in bout number. Western immunoblot revealed some minor leakiness of TDP-43 expression in the absence of RU, and even this low level of TDP-43 was associated with truncated sleep bout length during the day (Fig. 3, A and F). Overall, the degree of sleep loss leveled off at 0.5 mM RU486, driven by effects on sleep bout length; therefore, we used this dosage for subsequent experiments.

Atx2 knockdown normalizes TDP-43–associated sleep disruptions

Concurrent up-regulation of *Atx2* and TDP-43 in *Drosophila* worsens retinal degeneration and severely truncates lifespan, beyond that of expressing TDP-43 (or *Atx2*) alone (*58*). Moreover, genetic reduction of *Atx2* ameliorates TDP-43 toxicity in *Drosophila* and

mitigates toxicity and cellular inclusions in mouse models (*59*). The ability of TDP-43 to bind RNA is important for its toxicity, and the Atx2 polyA-binding protein interacting motif (PAM) domain is critical for its ability to enhance TDP-43 toxicity (*58*, *70*). Given these interactions for toxicity, we examined sleep in TDP-43–expressing animals while manipulating *Atx2* levels. To assess the impact on sleep of *Atx2* up-regulation, we used the *Da*GS driver to express both UAS-*TDP-43*^{52S} and UAS-*Atx2*.1B; however, all flies died within 2 days of being placed on RU486, precluding sleep analysis. We then asked whether RNA interference (RNAi)–mediated knockdown of *Atx2* ameliorates the sleep deficits observed in *Da*GS>UAS-*TDP-43*^{52S}. Using this approach with three distinct RNAi lines for *Atx2* knockdown, we observed a twofold increase in total sleep time, driven by extension of sleep bout duration (Fig. 4, A to G). The *Atx2* RNAi line showing strongest knockdown (fig. S5A) was also associated with the largest sleep increase in TDP-43 flies, rescuing back to control levels (fig. S5B). *Atx2* RNAi expression in the absence of TDP-43 did not affect sleep, indicating a specific interaction between *Atx2* RNAi and TDP-43 for sleep recovery (Fig. 4H). These data reveal that the sleep deficits associated with TDP-43 expression are rescued by reduction of *Atx2*.

Small-molecule metabolic pathways mediate *Atx2* RNAi rescue of TDP-43 sleep disruption

To gain insight into molecular pathways by which *Atx2* modulates sleep in TDP-43–expressing animals, we performed RNA-seq analysis from brains of animals expressing TDP-43 with or without *Atx2* RNAi, along with corresponding control brains (Fig. 5, A and B, and

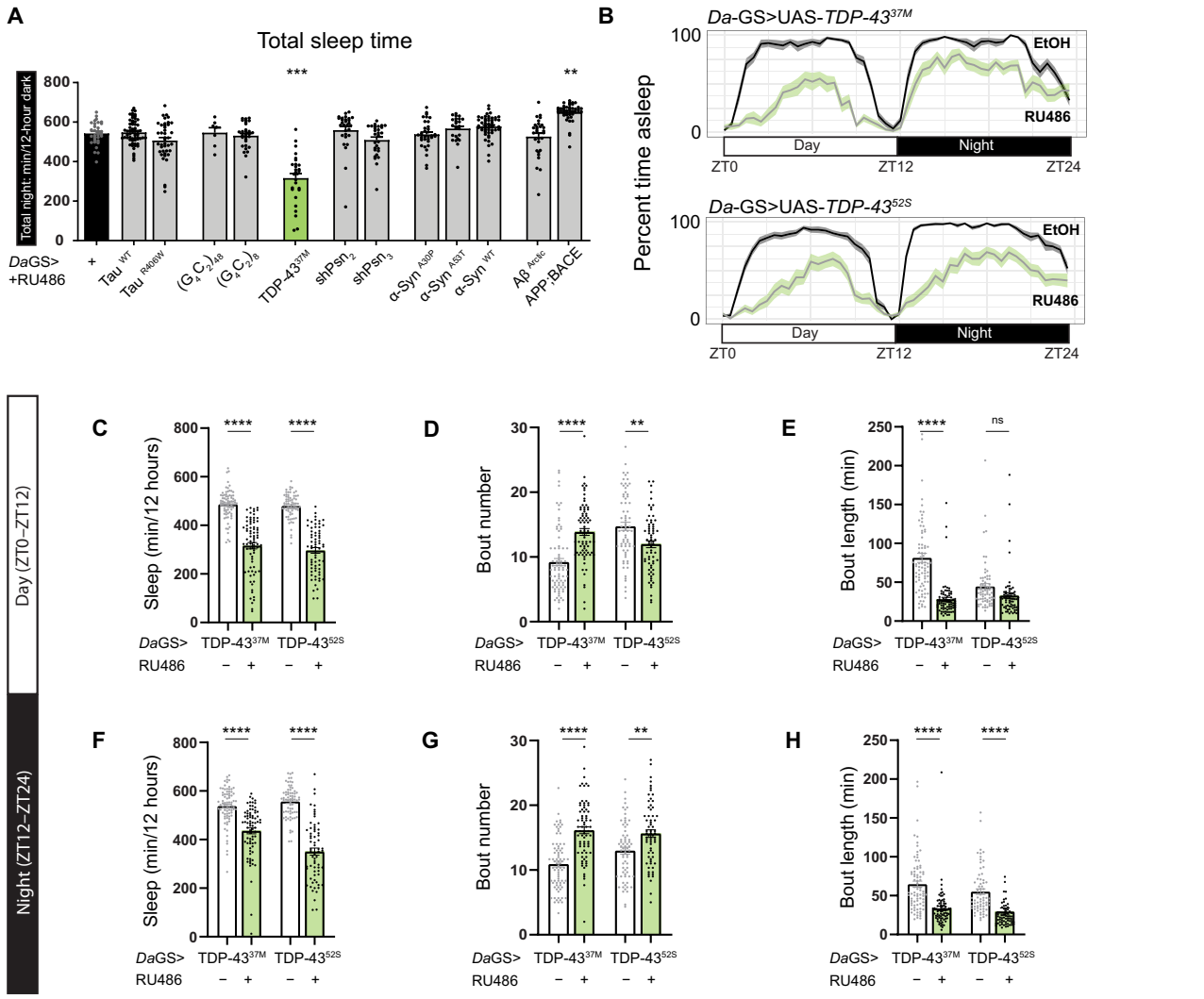

Fig. 1. Expression of human TDP-43 disrupts sleep in *Drosophila*. (**A**) Screen of sleep phenotypes in gene expression models of neurodegenerative disease. *Da*GS on RU486 food. Quantification of total sleep time during the dark (night) phase (from left to right, $n = 32, 60, 41, 7, 31, 28, 29, 29, 34, 25, 50, 30$, and 44 flies). (**B**) Sleep traces of TDP-43 flies on ethanol (black traces) or RU486 (green traces) after 7 days. (**C** to **E**) Quantification of day sleep duration (C), sleep bout number (D), and sleep bout length (E) for TDP-43 flies ($n > 32$ flies per condition). (**F** to **H**) Quantification of night sleep duration (F), bout number (G), and bout length (H) ($n > 32$ flies per condition). In (C) to (H), $n = 80, 77, 69$, and 67 from left to right. For all figures, error bars represent SEM; $^{**}P < 0.01$, $^{***}P < 0.001$, and $^{****}P < 0.0001$ by one-way analysis of variance (ANOVA) with Dunnett's multiple comparisons test (A) or Sidak's multiple comparisons test [(C) to (H)].

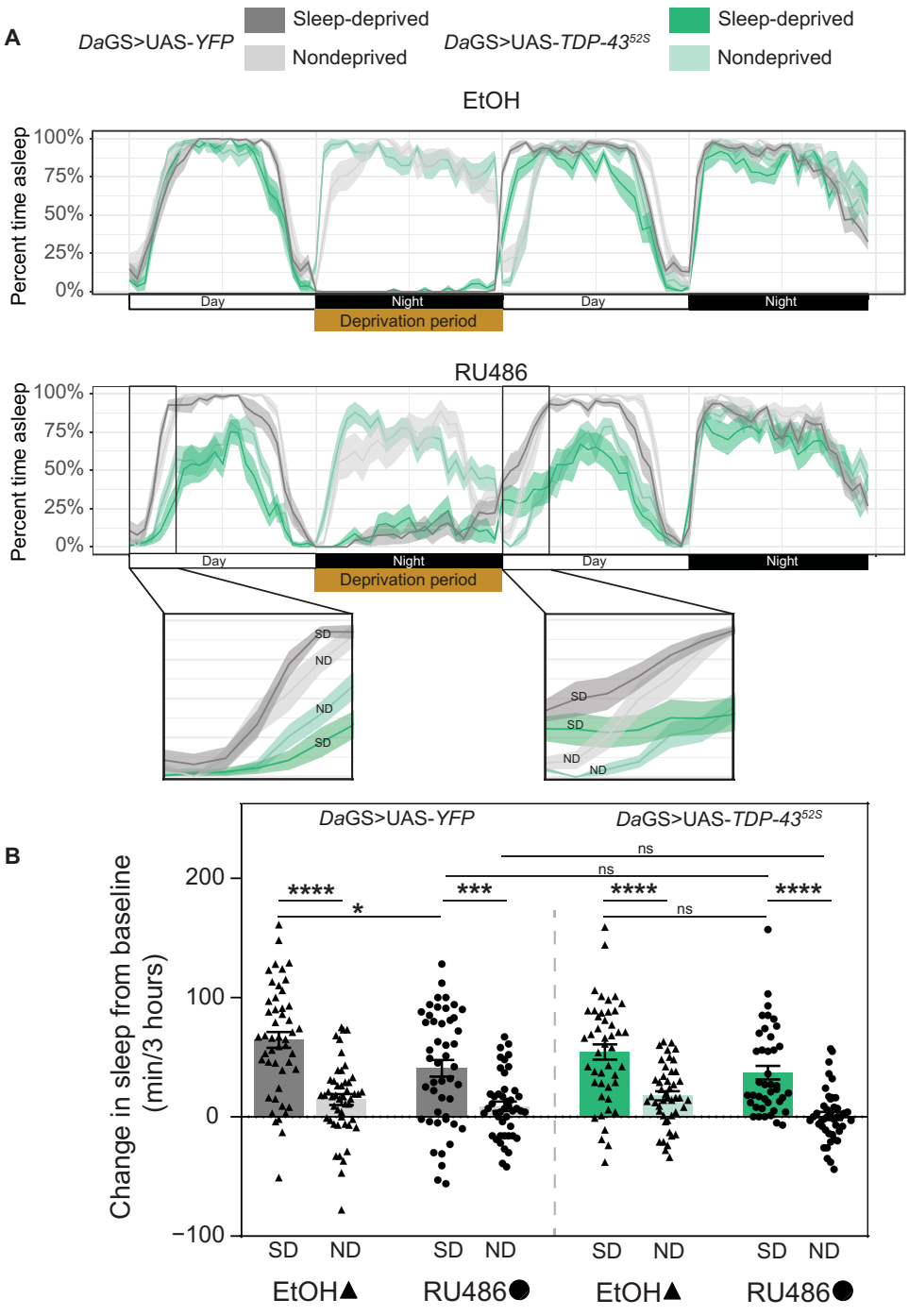

Fig. 2. TDP-43–expressing flies maintain the homeostatic sleep response following sleep deprivation. (**A**) Sleep traces of TDP-43 and control flies before, during (indicated by orange bar), and after 12-hour sleep deprivation. Top traces are those raised on ethanol, and bottom traces are raised on RU486. (**B**) Quantification of the change in total sleep time from baseline recording (first 3 hours of daytime before deprivation) to recovery sleep recording (first 3 hours of daytime after deprivation). From left to right, $n = 48, 48, 47, 45, 45, 45, 41$, and 43. $^{*}P < 0.05$, $^{***}P < 0.001$, and $^{****}P < 0.0001$ by three-way ANOVA with Sidak's multiple comparisons. Significant effects of deprivation [sleep-deprived (SD) versus nondeprived (ND), $P < 0.0001$] and treatment [RU486 versus ethanol (EtOH), $P < 0.0001$] were detected. No significant effects of genotype nor significant interactions between factors (genotype, treatment, and deprivation) were detected.

data S2). *Da*GS>UAS-*TDP-43*^{52S} flies survive to ~9 to 10 days at 25°C (starting RU486 immediately after eclosion) compared to a normal lifespan of ~60 to 70 days, validating a severe toxicity of TDP-43 expression. RNA-seq on brain tissue was performed after 6 days on RU486 at 50% survival (Fig. 5C). Flies ubiquitously expressing TDP-43 with *Atx2* RNAi had a slightly increased overall lifespan, with a 50% survival at 8 days and total lifespan of ~11 to 12 days (Fig. 5C).

Upon TDP-43 expression, 3295 transcripts were differentially expressed within the brain, with ~50% (1657) of these up-regulated (Fig. 5D). Transcripts up-regulated in TDP-43 brains were enriched for pathways such as small-molecule metabolic processing and mitogen-activated protein kinase (MAPK) signaling, suggesting that metabolic and stress signaling were activated in response to TDP-43 (Fig. 5E and data S3). We analyzed gene changes in TDP-43 brains compared to TDP-43 brains with *Atx2* RNAi, when sleep is rescued. We considered that crucial pathways of toxicity up-regulated by TDP-43 might be subsequently down-regulated by *Atx2* knockdown, prompting protection. Our analysis revealed that 396 transcripts were up-regulated with TDP-43 but now

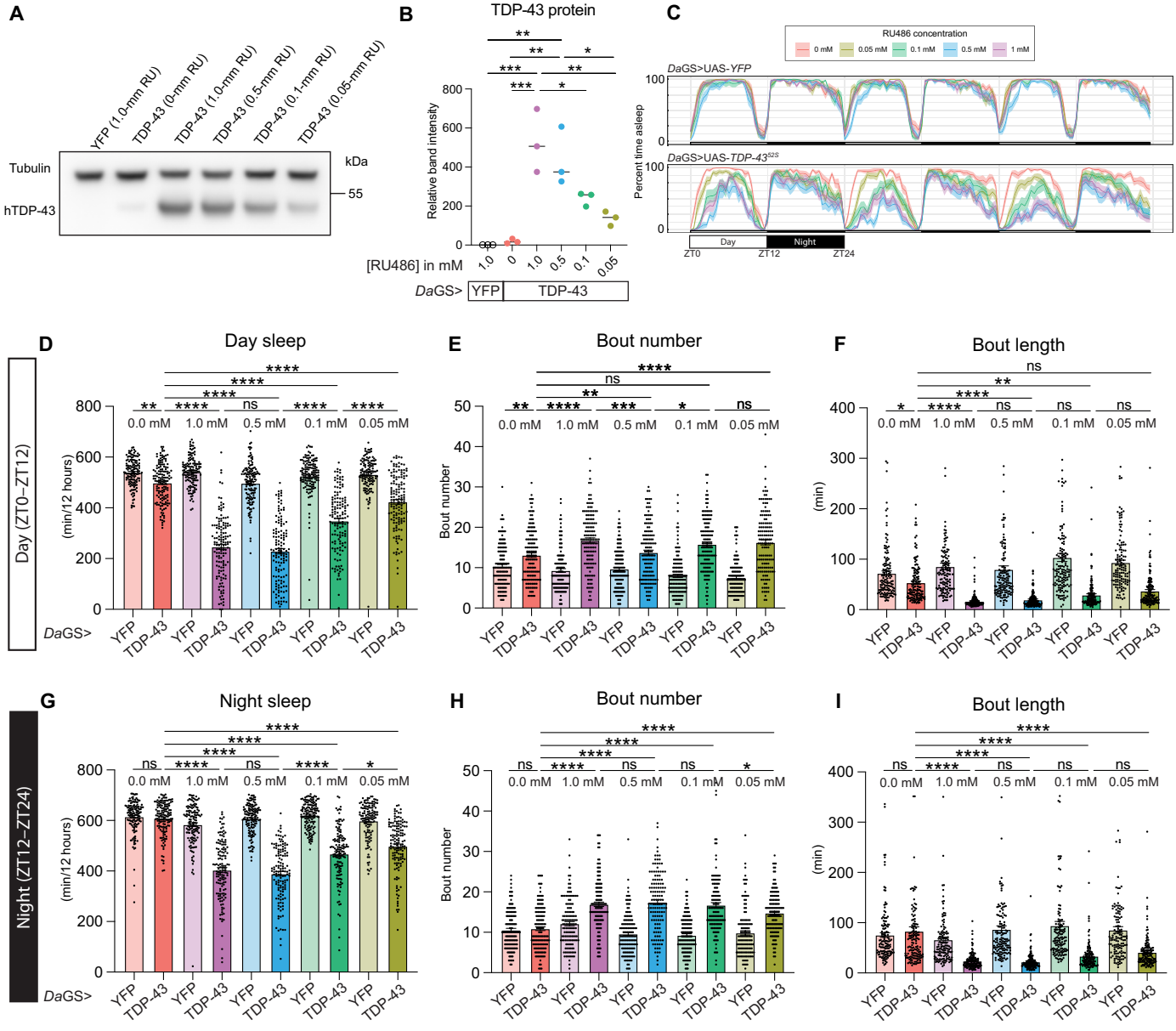

Fig. 3. Dose-dependence of TDP-43 sleep phenotypes. (**A**) Western immunoblot of TDP-43 protein from fly heads following 6 days on different concentrations of RU486. $n = 10$ heads per protein sample, 3 biological replicate blots quantified. (**B**) Quantification of relative band intensity for TDP-43 protein normalized to tubulin control. (**C**) Sleep traces over three consecutive days for flies at 6 to 8 days on varying concentrations of RU486. (**D** to **F**) Quantification of day sleep time (D), bout number (E), and bout length (F) for flies raised on varying RU486 concentrations ($n > 32$ flies per condition). (**G** to **I**) Quantification of night sleep time (G), bout number (H), and bout length (I) for flies raised on varying RU486 concentrations. For (D) to (I), from left to right, $n = 144, 138, 141, 129, 138, 141, 134, 141, 138$, and 135. $^*P < 0.05$, $^{**}P < 0.01$, $^{***}P < 0.001$, and $^{****}P < 0.0001$ by one-way ANOVA with Tukey's multiple comparisons test (B) or one-way ANOVA with multiple comparison Sidak's test [(D) to (I)].

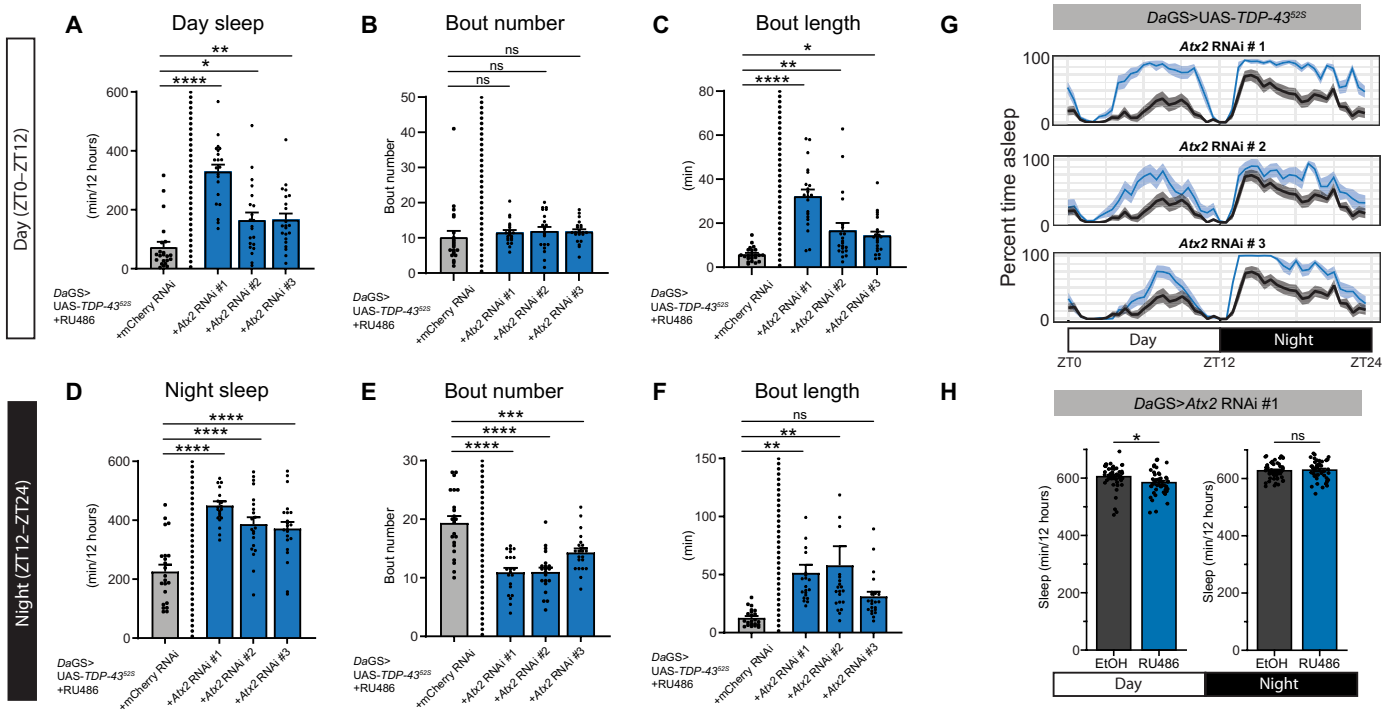

Fig. 4. *Atx2* knockdown suppresses TDP-43 sleep phenotypes. (**A** to **C**) Quantification of day sleep time (A), bout number (B), and bout length (C) for TDP-43 flies with or without *Atx2* knockdown. (**D** to **F**) Quantification of night sleep time (D), bout number (E), and bout length (F) for TDP-43 flies with or without *Atx2* knockdown. From left to right, $n = 22$, 21, 21, and 22. $^*P < 0.05$, $^{**}P < 0.01$, $^{***}P < 0.001$, and $^{****}P < 0.0001$; ns, not significant by one-way ANOVA with Dunnett's multiple comparisons to *Da*GS>UAS-mCherry RNAi control [(A) to (F)]. (**G**) Sleep traces of *Da*GS>UAS-*TDP-43*^{52S} flies, also expressing *Atx2* RNAi after 5 days on RU486. (**H**) Quantification of sleep time of *Da*GS>*Atx2* RNAi #1 flies after 5 days on RU486. $n = 47$ and 45 for EtOH and RU486 conditions, respectively. $^*P < 0.05$ by unpaired *t* test with Welch's correction.

down-regulated in TDP-43 brains coexpressing *Atx2* RNAi (Fig. 5F); most of these transcripts were not normally down-regulated by *Atx2* RNAi alone (fig. S5, C and B). These transcripts were significantly enriched for small-molecule metabolic processing and catabolic processing pathways (Fig. 5G and data S3), suggesting that TDP-43 brains undergo transcriptional activation in metabolic processing pathways that is reduced upon *Atx2* RNAi. Dysregulation of metabolic pathways has been implicated in the pathogenesis of both ALS and sleep disorders (*50*, *71*–*74*), and *Atx2* may exert a protective effect in TDP-43 brains by regulating metabolic processing.

RNAi-based screen identifies additional metabolic sleep modifiers of TDP-43

The above findings raised the possibility that one or more of the genes whose expression level was normalized or down-regulated by *Atx2* RNAi may be of special importance, such that knockdown of the gene on its own could rescue TDP-43–associated sleep loss. We screened over 200 RNAi lines targeting genes that followed this expression pattern to determine whether knockdown of any could rescue the TDP-43 sleep phenotype, as observed with *Atx2* knockdown (Fig. 6, A and B). TDP-43 flies typically sleep ~500 min across the 24-hour day. Of the lines screened, 50 were able to suppress the TDP-43 sleep phenotype to at least some extent, being associated with >700 min of total sleep (Fig. 6C and data S4). These modifier genes overlapped with the previous gene ontology (GO) term pathway genes of small-molecule metabolic processing (Fig. 6C); dysregulation of key metabolic pathways may therefore play a crucial role in sleep loss of TDP-43 flies. Sleep modifiers regulating metabolic processing included *Myc* (drives expression of genes in glycolysis and tricarboxylic acid cycle), *InR* (promotes uptake and storage of glucose, insulin signaling), and *Atg1* [role in autophagy, and interacts with adenosine monophosphate-activated protein kinase (AMPK), mammalian target of rapamycin (mTOR), and glycogen synthesis pathways]. These genes were all up-regulated upon TDP-43 expression and then down-regulated upon coexpression of *Atx2* RNAi, but not affected by *Atx2* RNAi at baseline (Fig. 6D). Knockdown of each gene independently also suppressed the TDP-43 sleep phenotype (Fig. 6, E and F). Among these, *Atg1* RNAi showed the greatest rescue in overall sleep (day + night), with a total sleep of ~800 min, comparable to *Atx2* RNAi sleep recovery (~900 min) (Fig. 6, E and F, and data S4).

TDP-43–expressing brains exhibit glycogen metabolism dysfunction

Given the marked effect of TDP-43 on *Atg1* expression levels and rescue of TDP-43 sleep phenotypes with *Atg1* knockdown, we next explored these interactions in more depth. Comparing to additional controls, we found knockdown of *Atg1* in TDP-43 flies rescued sleep duration during the day and night, as well as normalizing measures of sleep fragmentation (fig. S6, A and B). *Atg1* knockdown also extended survival of TDP-43–expressing flies to a similar extent as *Atx2* RNAi (Fig. 7A). Consistent with published work (*75*), knockdown of *Atg1* alone was associated with an increase in sleep duration (fig. S6B). Knockdown of *Atg1* RNAi did not alter the levels of

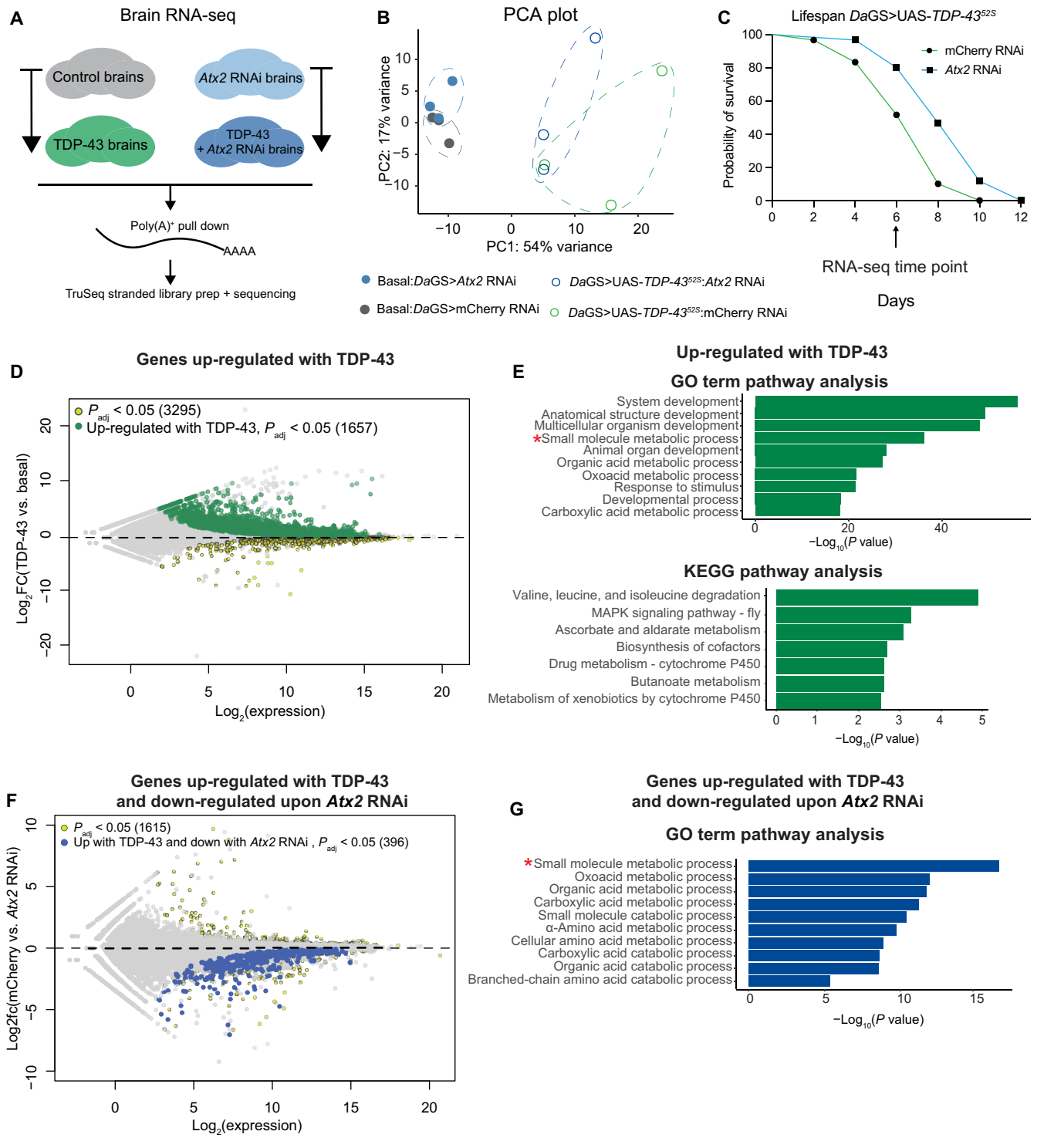

Fig. 5. Mechanistic insight from RNA-seq of TDP-43 brains ± *Atx2* RNAi. (**A**) Schematic of RNA-seq experimental design. Brains from *Da*GS>UAS-*TDP-43*^{52S} × mCherry RNAi or *Da*GS>UAS-*TDP-43*^{52S} × *Atx2* RNAi were sequenced after 6 days on RU486. Poly (A)$^{+}$, polyadenylated. (**B**) Principal components analysis (PCA) plot of RNA-seq data. PC1 reflects TDP-43 expression, with *Atx2* RNAi samples being shifted toward controls relative to TDP-43 expression only. (**C**) Lifespan analysis of *Da*GS>UAS-*TDP-43*^{52S} with *Atx2* RNAi. $n = 60$, ****$P < 0.0001$ log-rank test. (**D**) MA plot of genes altered in TDP-43–expressing brains. Light blue marks all differentially expressed genes $P_{adj} < 0.05$ (3295 genes), and green overlay highlights significantly up-regulated transcripts (1657) $P_{adj} < 0.05$. (**E**) Gene ontology (GO) term and Kyoto Encyclopedia of Genes and Genomes (KEGG) pathway analysis of genes up-regulated in TDP-43 brains. (**F**) MA plot of genes differentially expressed in brains of animals expressing TDP-43 and *Atx2* RNAi. Light blue indicates all differentially expressed genes (1615) $P_{adj} < 0.05$, whereas dark blue marks genes that were significantly up-regulated with TDP-43 that are now down-regulated with *Atx2* RNAi $P_{adj} < 0.05$ (396). (**G**) GO term analysis of the 396 genes that were up-regulated in TDP-43–expressing brains but that are now down-regulated with *Atx2* RNAi.

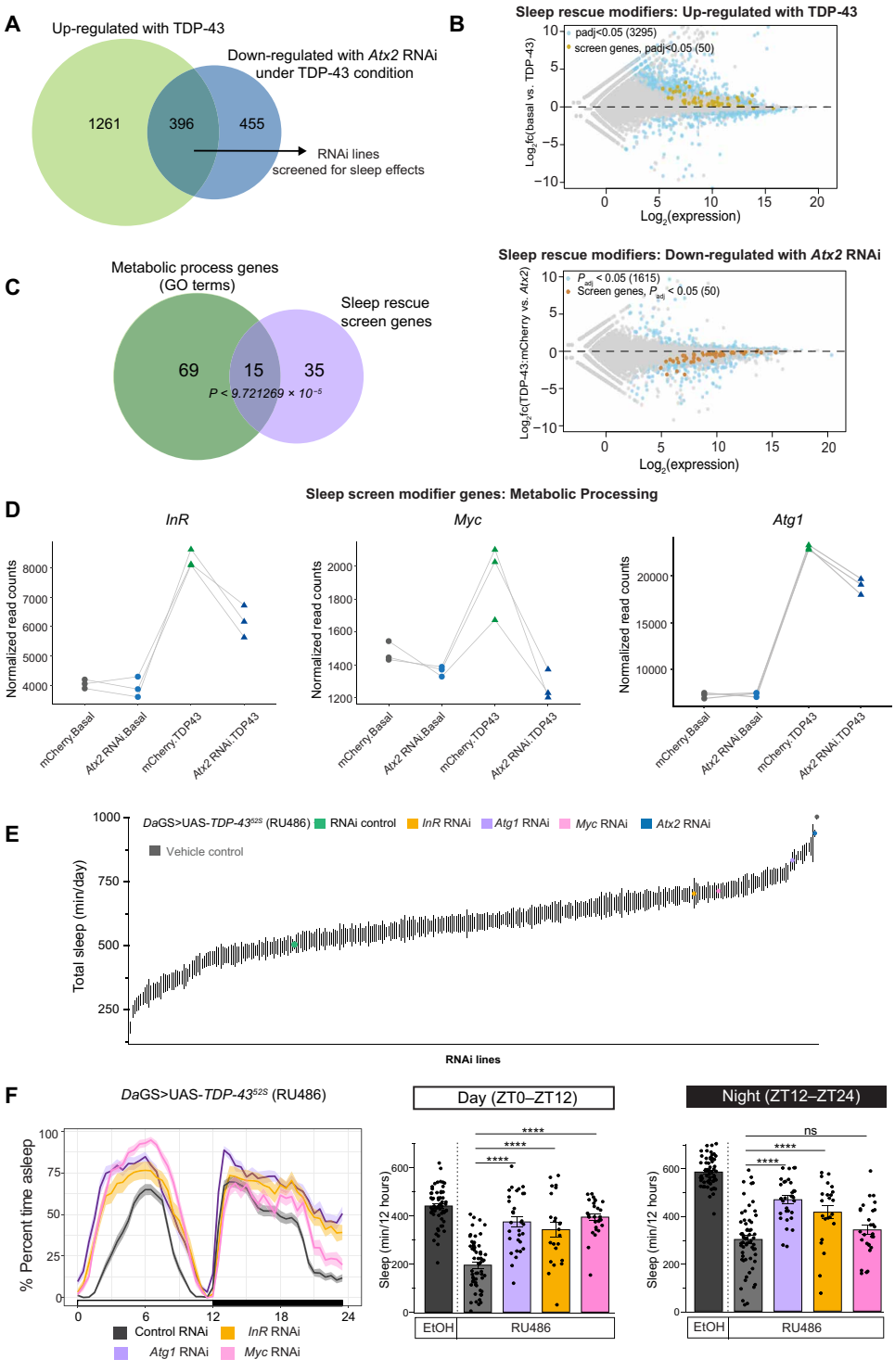

Fig. 6. Small-molecule metabolic pathways mediate *Atx2* RNAi rescue of TDP-43 sleep disruption. (**A**) Overlap of transcripts up-regulated in TDP-43 brains (1261 + 396), and transcripts down-regulated upon *Atx2* RNAi in TDP-43 brains. Genes to which there were available RNAi lines (224) were screened for their effects on sleep with TDP-43. (**B**) MA plot showing the sleep modifier genes (brown) are up-regulated upon TDP-43 expression and down-regulated with *Atx2* RNAi. (**C**) Genes from GO term analysis "small-molecule metabolic process" (see Fig. 5G) overlap with sleep rescue genes ($P < 9.721269 \times 10^{-5}$). (**D**) Normalized read counts of sleep modifier genes showing an increase with TDP-43 expression and a down-regulation with added *Atx2* RNAi. *InR*, *Myc*, and *Atg1* also enriched in small-molecule metabolic processing GO term. (**E**) Sleep screen of RNAi lines coexpressed with TDP-43 [green is TDP-43 with RNAi control; gray (far right) is baseline sleep]. (**F**) Sleep traces of TDP-43 flies + RNAi or control, on RU486, and quantification of sleep duration during the day and night. From left to right, $n = 58, 61, 31, 23$, and 28. ****$P < 0.0001$ by one-way ANOVA with Dunnett's multiple comparisons test.

TDP-43 (fig. S6C). *Atg1* canonical function is in the autophagy pathway, which is linked to sleep regulation (*75*) and can become dysfunctional in neurodegeneration (*76*, *77*). To explore the role of additional autophagy-related genes in TDP-43 sleep disturbances, we examined the impact of knocking down other autophagy pathway transcripts. Although knockdown of these genes independent of TDP-43 is known to increase sleep duration (*75*), RNAi expression in the context of TDP-43 did not rescue the sleep deficits (fig. S6D). None of these autophagy brain transcripts were altered upon TDP-43 expression (data S2). These findings raised the possibility that the function of *Atg1* RNAi in mitigating TDP-43 sleep phenotypes is not via a general autophagy pathway.

Additional roles of *Atg1* include glucose metabolism and insulin signaling through an interaction with AMPK and glycogen breakdown (*78*, *79*). Moreover, growing evidence in both patient and animal models suggests that dysfunctional energy metabolism plays a substantial role in progression of ALS, indicated by altered glucose utilization in specific brain and spinal cord regions (*51*, *71*, *72*, *74*). As pathways regulated by *Atx2* knockdown in the brain were enriched in metabolic processing, we considered whether there was a metabolic imbalance in TDP-43 brains that could be responsible for the sleep defect that is normalized by *Atx2* RNAi. Thus, we sought to examine small-molecule metabolic profiles by measuring glycogen/glucose levels in the brain. Although TDP-43 brains showed no significant change in steady state glucose levels, TDP-43 brains had increased glycogen storage levels compared to controls (Fig. 7B). *Atx2* RNAi and *Atg1* RNAi reduced glycogen levels, suggesting a more normal utilization of glycogen stores (Fig. 7B). Thus, brains from animals expressing TDP-43 are abnormal in their overall glycogen storage, and modifiers of the sleep phenotype correlated with reduction of glycogen levels. These findings highlight a dysregulation of energy metabolism with TDP-43 expression that becomes restored upon *Atx2* RNAi.

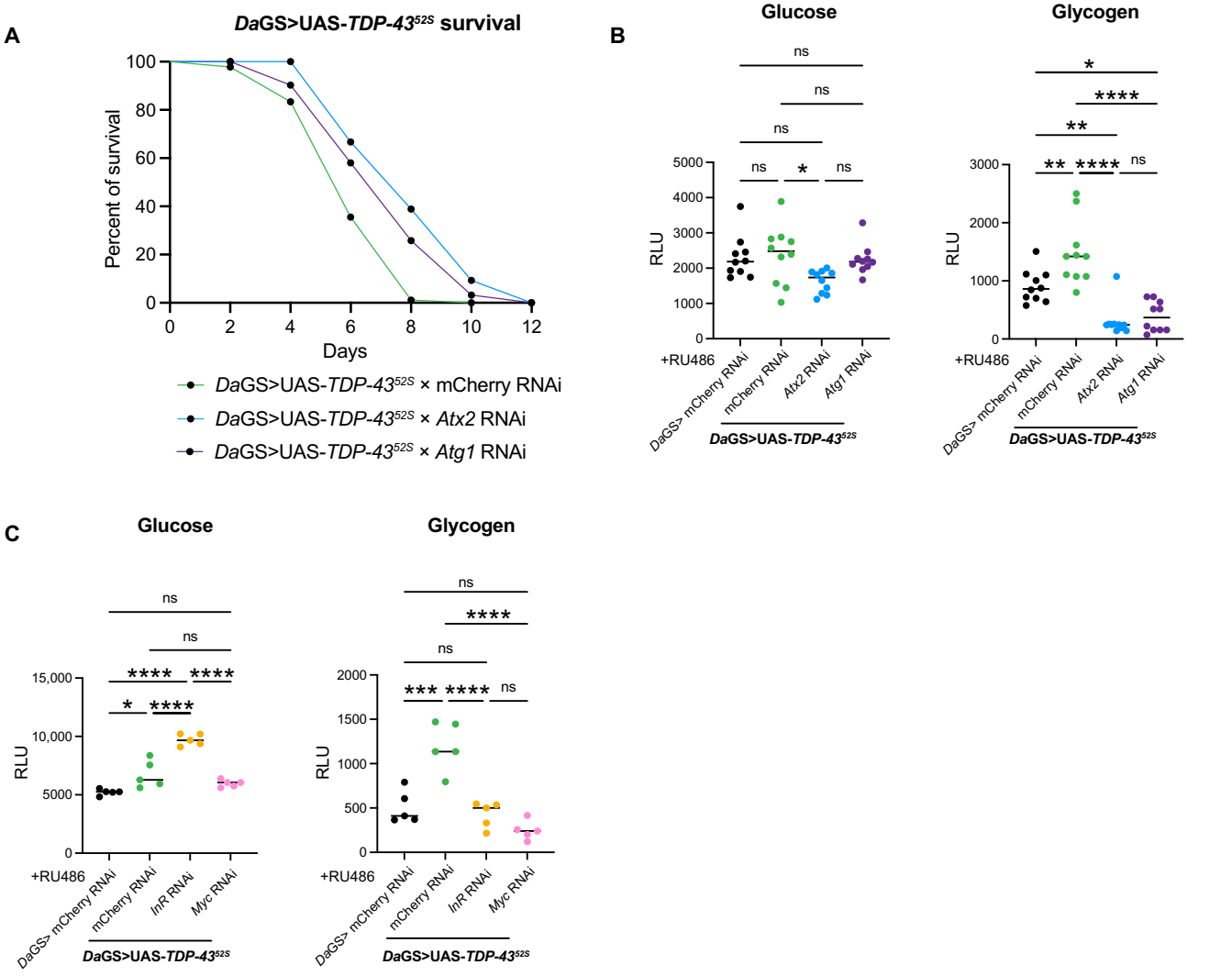

Fig. 7. *Atx2* and *Atg1* knockdown reduce glycogen storage dysfunction in TDP-43–expressing brains. (**A**) *Atg1* RNAi increased longevity of TDP-43–expressing flies, $n = 90$, 91, and 91, $^{****}P < 0.01$, log-rank test, comparable to that of *Atx2* RNAi. (**B**) TDP-43 brains have increased glycogen levels compared to control brains, and *Atx2* RNAi and *Atg1* RNAi reduce glycogen levels. $n = 9$ brains each point represents one brain, per genotype, $^{*}P < 0.05$, $^{**}P < 0.01$, and $^{****}P < 0.0001$, one-way ANOVA Tukey's multiple comparison test. RLU, relative light unit. (**C**) Additional metabolic transcripts such as *InR* RNAi and *Myc* RNAi also reduce glycogen levels. $n = 5$ brains per genotype, $^{*}P < 0.05$, $^{***}P < 0.001$, and $^{****}P < 0.0001$, one-way ANOVA Tukey's multiple comparison test.

We next tested additional key metabolic genes that were highly up-regulated with TDP-43 and normalized by *Atx2* RNAi, including *Myc* and *InR*; knockdown of these genes also attenuated TDP-43 sleep disruptions (see Fig. 4). We found that knockdown of *Myc* and *InR*, like *Atx2* and *Atg1*, was associated with reduced glycogen levels in TDP-43 brains (Fig. 7C). These findings further underscore that metabolic dysfunction is associated with the sleep loss phenotype in TDP-43 animals.

Rapamycin normalizes sleep-starvation and glycogen metabolic phenotypes in TDP-43 flies.

TDP-43–expressing animals are markedly stress sensitive, with a compromised ability to withstand heat stress and starvation stress (*80*). Upon starvation, wild-type flies normally suppress sleep to increase foraging for food (*81*). Given that TDP-43 flies have reduced sleep at baseline and are starvation sensitive, we considered that their sleep loss/fragmentation could be driven by a metabolic starvation condition reflected by the impaired glycogen utilization, even in the presence of adequate food resources. Consistent with this hypothesis, RNA-seq analysis indicated that key starvation-sleep–associated transcripts such as *Clk* and *for* (*81*) are up-regulated in TDP-43 brains (data S2). To test this idea further, we examined the sleep response to starvation in TDP-43 flies, focusing on the first 12 hours of starvation since previous work has shown that >80% of these flies die between 24 and 48 hours of starvation (*80*). While genetic and vehicle control flies exhibited the expected sleep suppression upon starvation, sleep loss was more severe in flies expressing TDP-43 (Fig. 8A). These findings support the hypothesis that a core metabolic dysregulation is critical in the sleep phenotype of TDP-43–expressing animals.

Rapamycin is a suppressor of TDP-43 toxicity in *Drosophila* for lifespan and locomotor deficits (*82*, *83*) and inhibits the activity of TOR, a major regulator of nutrient sensing and the insulin signaling pathway (*83*). Rapamycin also increases resistance to starvation stress (*84*). We therefore asked whether rapamycin could correct the sleep and metabolic deficits in TDP-43 flies. In control brains, rapamycin treatment caused an increase in glycogen levels, indicating a disruption in glucose/glycogen homeostasis in a basal brain (Fig. 8B). By contrast, in TDP-43 brains, rapamycin treatment decreased glycogen storage levels back to baseline, rescuing this metabolic imbalance (Fig. 8B).

We then assessed the impact of rapamycin on sleep. Rapamycin treatment alone of control animals resulted in a reduction in daytime sleep, while night sleep was unaffected (Fig. 8C). Therefore, we focused on the effect of rapamycin on nighttime sleep loss associated with TDP-43 and found that rapamycin treatment increased night sleep duration of TDP-43 animals (Fig. 8C). Last, we assessed whether rapamycin rescued the exaggerated sleep response to starvation in TDP-43 flies. Rapamycin treatment of starved TDP-43 animals markedly mitigated the sleep loss associated with starvation (Fig. 8D). Together, these data suggest that TDP-43 animals have a dysfunctional metabolic state that leads to sleep deficits; *Atx2* and several other metabolic genes, as well as rapamycin treatment, can mitigate the sleep loss of TDP-43 flies and restore glycogen balance.

DISCUSSION

Neurodegenerative diseases, such as FTD and ALS, are characterized by the progressive degeneration of neurons, leading to various cognitive impairments. Sleep disturbances are a prominent symptom in neurodegenerative disease and are thought to contribute to disease progression. In this study, we find that a fly model of ALS/FTD expressing TDP-43 exhibits a robust sleep disturbance, enabling a search for genetic modifiers. We elucidate the relationship between TDP-43 toxicity and *Atx2* knockdown in disease, revealing a reciprocal relationship in small-molecule metabolism along with recovery of sleep. Similarly, we identify additional TDP-43 sleep modifiers in metabolism genes regulated by *Atx2* knockdown. Starvation is a condition that drives sleep loss in normal animals (*81*), and TDP-43 animals are highly starvation stress sensitive (*80*). Our data show that TDP-43 flies also exhibit notable sensitivity to starvation-related sleep loss, and rapamycin restores glycogen metabolism and attenuates sleep loss under both baseline and starved conditions in TDP-43 flies. These data support a unifying model where sleep disturbances associated with TDP-43 are due to small-molecule metabolic dysregulation downstream of *Atx2* and highlight a therapeutic potential for rapamycin in targeting sleep (Fig. 9).

TDP-43–expressing flies exhibit severe sleep degradation

TDP-43 is a key protein associated with ALS pathology, and its aberrant mislocalization and aggregation have been implicated in neuronal dysfunction and degeneration (*46*, *85*–*87*). Our findings demonstrate that the expression of TDP-43 in the adult fly leads to severe sleep disruptions, characterized by reduced sleep duration and sleep fragmentation during both day and night. These data are consistent ALS patient sleep studies that show disrupted sleep (*14*, *15*, *88*). A key insight from our TDP-43 manipulation is the absence of locomotor deficits in sleep assays, eliminating this potential confound and suggesting that sleep disturbances are not coupled to the motor phenotypes. Knockdown of *Atx2*, a modifier of TDP-43 toxicity for motor dysfunction and lifespan (*58*, *59*), also rescues the sleep deficits induced by TDP-43 expression. These data highlight a crucial role for *Atx2* in regulating sleep disturbances associated with TDP-43 pathology.

We observed no effect on sleep homeostasis or circadian locomotor rhythms with TDP-43 expression, pointing toward a specific disruption of daily sleep duration and continuity. Previous studies have shown *ATXN2/Atx2* affects circadian rhythms and translation control (*89*–*91*). Given the lack of a circadian phenotype with TDP-43 expression in flies, it is unclear how the role of *Atx2* in circadian control might be linked to the TDP-43 sleep phenotype. One possibility is that TDP-43–related sleep deficits are related to *Atx2* effects on translation at specific times of day, perhaps through *Myc*, *Atg1*, or *Inr*. Regardless, we establish a relationship between TDP-43 expression and sleep deficits, with higher levels of TDP-43 protein leading to increased sleep loss; notably, even low levels of TDP-43 were sufficient to induce fragmented sleep patterns, with a marked reduction in the length of sleep bouts. The extreme sensitivity of sleep continuity to TDP-43 levels raises the possibility that sleep fragmentation might represent an early and sensitive marker of this degenerative process. Prospective sleep assessments in human populations will be of great importance to explore this idea directly.

To gain insight into the underlying mechanisms of the sleep disruptions, we performed RNA-seq analysis on the brains of flies expressing TDP-43 with or without *Atx2* knockdown. Our analysis highlighted alterations in gene expression related to small-molecule metabolism pathways in TDP-43–expressing flies. Notably, these metabolic pathways were restored to near-normal levels upon *Atx2*

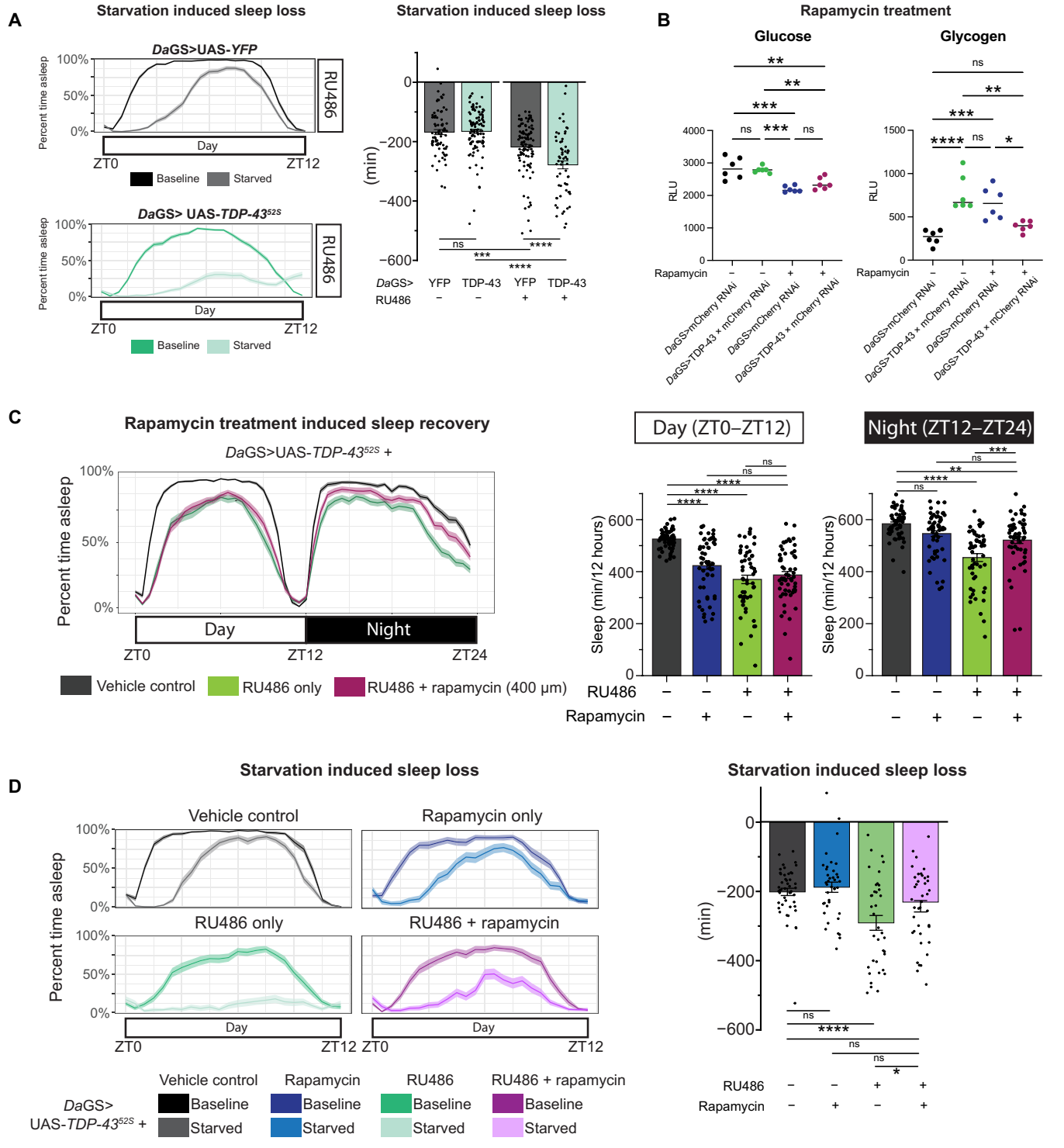

Fig. 8. Rapamycin normalizes sleep-starvation and glycogen metabolic phenotypes in TDP-43 flies. (**A**) Sleep traces of TDP-43 flies and genetic controls on RU486 at baseline and in the absence of food and quantification of sleep loss in the absence of food for these flies and vehicle controls. From left to right, $n = 82$, 114, 110, and 68. ***$P < 0.001$ and ****$P < 0.0001$ by one-way ANOVA with Sidak's multiple comparisons test. (**B**) Treatment of flies + RU486 with or without rapamycin (400uM) for 6 days in food. *Da*GS × mCherry RNAi, *Da*GS>UAS-*TDP-43*^{52S} × mCherry RNAi. Rapamycin-treated animals show reduced glucose and glycogen levels, $n = 6$ brains per genotype, **$P < 0.01$, ***$P < 0.001$, and ****$P < 0.0001$, one-way ANOVA Tukey's multiple comparison test. RLU, relative light unit. (**C**) Sleep traces of TDP-43 flies and those on RU486 alone or with rapamycin and quantification of sleep duration during the day and night for each condition. From left to right, $n = 57$, 58, 54, and 57. **$P < 0.01$, ***$P < 0.001$, and ****$P < 0.0001$ by one-way ANOVA with Tukey's multiple comparisons test. (**D**) Sleep traces of TDP-43 flies at baseline and in the absence of food on vehicle control, RU486, rapamycin, or both and quantification of sleep loss in the absence of food for these flies. From left to right, $n = 47$, 37, 29, and 37. *$P < 0.05$ and ****$P < 0.0001$ by one-way ANOVA with Tukey's multiple comparisons test.

knockdown. These data suggest an involvement of metabolic dysregulation in TDP-43–induced sleep disturbances. Analysis of plasma metabolome after sleep restriction in humans reveals that small molecule and amino acid metabolism are particularly perturbed (*73*). In accordance with our RNA-seq analysis, we hypothesize human plasma may reveal similar metabolic signatures in patients with ALS. Notably, *Atx2* RNAi did not alter sleep levels in control flies, indicating that *Atx2* regulates sleep specifically in pathways that are dysregulated with TDP-43.

Several other genes regulated by *Atx2* RNAi also ameliorated sleep disturbances associated with TDP-43, with *Atg1* RNAi showing the most robust improvement in sleep duration among these modifiers. Although *Atg1* is known for its role in autophagy and autophagy dysregulation is implicated in both neurodegeneration and sleep (*75*, *92*), screening additional autophagy pathway genes showed no effect on the TDP-43 sleep phenotype. These data point toward an autophagy-independent role affecting TDP-43 sleep.

Metabolism in neurodegeneration and sleep

ALS pathology has been linked to dysregulation in glycogen metabolism and is associated with increased oxidative stress and impaired cellular energy balance (*50*, *74*, *93*). Recent reports have observed increased levels of glycogen in the lumbar spinal cord of ALS model SOD1^{G93A} mice (*53*). This impairment persists throughout the course of disease and is due to altered levels of phosphorylase B or the enzyme that degrades glycogen (*53*). Similar results were found in spinal cord tissue of patients with ALS, confirming that glycogen accumulation is a feature of the human disease (*52*). In our study, we observed elevated levels of glycogen in the brains of TDP-43–expressing flies, indicating disrupted glycogen storage and metabolism in these animals. Knockdown of *Atx2* or *Atg1* led to a reduction in glycogen levels, suggesting their involvement in regulating glycogen metabolism in the context of TDP-43 toxicity. These findings provide further evidence linking TDP-43 expression to glycogen storage and metabolism issues in ALS and highlight the role of *Atx2* as a modifier of both the glycogen dysregulation and sleep disturbances.

Atx2 reduction is neuroprotective for ALS across different model systems, with current efforts focused on understanding the mechanistic role in disease progression. Global proteome and metabolome profiling of *Atxn2*-KO mice cerebellum and liver shows that *Atxn2* depletion modulates nutrition and basal metabolism, such as branched chain amino acid metabolism, fatty acid metabolisms, and citric acid cycle (*94*). Spinocerebellar ataxia 2 patients, with elevated levels of ATXN2, show depleted levels of subcutaneous fat storage before motor deficits appear (*95*). In addition, mice with *Atxn2*

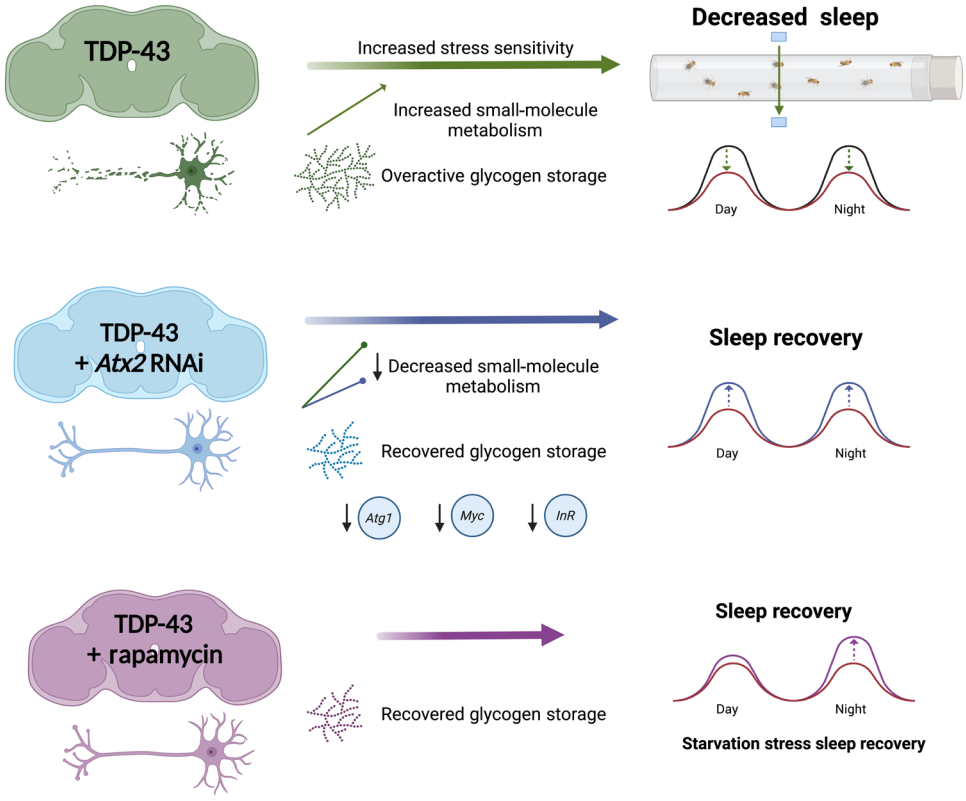

Fig. 9. Model for sleep disruption and rescue in TDP-43–expressing animals. TDP-43 expression in *Drosophila* causes a severe sleep phenotype that is rescued by *Atx2* RNAi. RNA-seq of TDP-43 brains with or without *Atx2* RNAi reveals up-regulation of small-molecule metabolism pathways, and these pathways were reduced upon *Atx2* knockdown. Analysis of metabolites revealed increased glycogen storage in TDP-43 brains, which was reduced with *Atx2* RNAi. Metabolism transcripts revealed from GO term analysis, such as *Atg1*, *Myc*, and *InR,* were up-regulated in TDP-43 brains and reduced with *Atx2* RNAi. Knockdown of these transcripts also recovered sleep and glycogen storage levels in TDP-43 flies. Similarly, treatment with rapamycin promoted sleep recovery in TDP-43 flies and restored glycogen levels. Rapamycin treatment restored starvation induced sleep loss of TDP-43 flies. This figure was made using http://BioRender.com.

deficiency have increased obesity and insulin resistance (*96*). Similarly, in *Drosophila, Atx2* knockdown in the larval fat body leads to developmental death and reduced growth, due to lipid breakdown deficiency (*97*). Furthermore, during periods of starvation stress, *Atx2* is activated via mTOR signaling pathway and localizes to stress-induced cytoplasmic granules to assist in stress resolution (*98*). During periods of stress, TDP-43 can also localize to stress granules where it may interact with Atx2, and accumulation of TDP-43 in the cytoplasm during disease progression makes the animals severely stress and starvation sensitive (*46*, *47*, *80*). Our study indicates that *Atx2* depletion is beneficial for the highly stress sensitive TDP-43 animals through the recovery of metabolism and sleep deficits. In the brain RNA-seq analysis, *Atx2* RNAi markedly normalized small-molecule metabolism defects that were up-regulated upon TDP-43 expression. Although TDP-43 animals with *Atx2* RNAi still die early because of the severe toxicity of TDP-43, the sleep disruption and brain glycogen levels are normalized. Future work will leverage these insights to understand whether and how brain degeneration and sleep are directly coupled, potentially examining cell type–specific regulation of TDP43 sleep disruption and guiding sleep-based therapies for neurodegenerative disease.

Rapamycin treatment has been shown to rescue the lifespan of TDP-43–expressing animals (*82*). By inhibiting TOR, rapamycin promotes a shift toward catabolism, autophagy, lipid breakdown, and energy conservation—processes that are beneficial in stress states (*82*, *84*). Although rapamycin rescues aspects of TDP-43 toxicity due to activation of autophagy pathways (*82*), in the sleep response, we find no role for most canonical autophagy genes and propose that rapamycin promotes metabolic and starvation recovery for TDP-43–related sleep disturbances. Rapamycin treatment restored the night sleep deficit associated with TDP-43, although sleep normalization was more complete with *Atx2* RNAi and additional players such as *Atg1*, *Myc*, and *InR* RNAi. This may be due to rapamycin treatment functioning only in part of the small-molecule metabolism signaling cascade. With starvation, TDP-43 flies showed enhanced suppression of sleep, likely primed by their chronic metabolic dysregulation. This exaggerated suppression of sleep was also mitigated by rapamycin. Elucidating the molecular pathways by which rapamycin impinges upon starvation stress (*84*) will provide insight into the ability of rapamycin to rescue TDP-43 toxicity. Together, these findings raise the intriguing possibility that baseline sleep disturbances related to TDP-43 might result from metabolic impairments that mimic a starvation-like state.

MATERIALS AND METHODS

Fly strains

Iso^{31} and *Daughterless*-GS flies were obtained from A. Sehgal (University of Pennsylvania). UAS:*Aβ Arctic* flies were obtained from M. Wu (Johns Hopkins). Lines were outcrossed at least 5× into the *iso*^{31} background. *Elav*-Gal4 (#458) and all RNAi lines were obtained from the Bloomington *Drosophila* Stock Center (see data S1 for a full list of lines). Flies were maintained on standard yeast/cornmeal-based medium at 25°C on a 12-hour:12-hour light:dark cycle.

RU486 food preparation and lifespan assay

To prepare a 50 mM stock solution, 215 mg of RU486 (Thermo Fisher Scientific) was dissolved in 10 ml of 100% ethanol (EtOH). One hundred milliliters of standard food or sucrose agar was melted, and 1 ml of RU486 or EtOH was added and mixed once cooled. Molten solution was poured into empty polystyrene vials (Genessee Scientific) or used to fill DAM tubes (Trikinetics). For lifespan analysis, food was prepared with either 100 μl of RU486 (4 mg/ml in 100% ethanol; Sigma-Aldrich, M8046-1G) pipetted onto food vials and allowed to dry for 24 hours. For lifespan analysis, adult male flies were collected at eclosion and aged on RU486, and flies were flipped to fresh food vials every 2 days. The number of dead/censored flies was recorded after flipping, and flies were housed at 25°C on a 12-hour light-dark cycle.

Rapamycin treatment

Rapamycin (LC laboratories) was prepared similar to RU486 food, at a concentration of 400 μM. Flies were treated with rapamycin + RU486 or RU486 alone for 6 days before metabolic testing or sleep analysis.

Sleep analysis

Male flies were collected at 1 to 3 days old and aged in group housing. Flies were then anesthetized on CO_2 pads (Genesee Scientific, catalog no. 59-114) and loaded into glass tubes containing 5% sucrose and 2% agar and RU486/rapamycin or EtOH as described above. All data collection began at ZT0 at least 24 hours following CO_2 anesthesia. Locomotor activity was monitored using the DAM system (Trikinetics, Waltham, MA). Activity was measured in 1-min bins, and sleep was defined as 5 min of consolidated inactivity (*99*). Data were processed with a custom R script using Rethomics package (*100*). Activity index was calculated as the average number of beam breaks per minute of wake time. For all experiments, the first day of data following loading was discarded. For starvation-induced sleep loss experiments, flies were monitored for baseline sleep and then transferred at ZT0 (lights on) into tubes containing only 2% agar and RU486/rapamycin or EtOH. Sleep loss for each fly was calculated as the difference between baseline sleep duration during the first 12 hours (ZT0 to ZT12) of the day preceding starvation and sleep duration during the first 12 hours immediately following transfer into tubes without food.

Sleep deprivation and homeostasis analysis

Male flies were collected, aged, and loaded onto either RU486 or EtOH as described above. Locomotor activity was monitored using the DAM system. Mechanical sleep deprivation was performed using a Trikinetics vortexer mounting plate. Monitors were shaken for 2 s randomly within every 20-s window for 12 hours during the night following 7 days on RU486. Rebound sleep was calculated as the difference between baseline sleep duration during the first 3 hours of the day (ZT0 to ZT3) preceding deprivation (7 days on RU486) and rebound sleep during the first 3 hours of the day immediately following nighttime deprivation (8 days on RU486).

Circadian rhythm analysis

Male *Da*GS>UAS-*TDP-43* and *Da*GS>UAS-*YFP* flies were loaded into the DAM system on RU486 or EtOH as described above and entrained to a 12-hour:12-hour light:dark cycle for 3 days before being transferred to constant darkness (DD). Locomotor activity during 6 to 8 days on RU486 (days 3 to 5 in DD) was analyzed in ClockLab software (Actimetrics, Wilmette, IL). Fast Fourier transform (FFT) was performed for the locomotor activity collected

during DD, and the maximum amplitude of the FFT was calculated and compared across genotype and condition. FFT values of >0.01 were considered rhythmic. Period length was calculated for all rhythmic flies (table S1).

RNA sequencing

*Da*GS>UAS-*TDP-43*^{52S} × mCherry RNAi and *Da*GS>UAS-*TDP-43*^{52S} × *Atx2* RNAi fly brains were dissected after 6 days on RU486 food. $n = 4$ biological replicates, 10 to 12 brains per sample. Tissue was homogenized in 200 μl of TRIzol (Thermo Fisher Scientific, 15596026) in ribonuclease-free 1.5-ml microfuge tubes (Thermo Fisher Scientific, AM12400). A total of 800 μl of TRIzol (Thermo Fisher Scientific, 15596026) was added to the tube, and 200 μl of chloroform (Thermo Fisher Scientific, AC423555000) was vigorously shaken for 20 s at room temperature. Samples were left for 5 min at room temperature to form upper aqueous phase and centrifuges at 4°C for 15 min at 12,000*g*. The upper aqueous phase was transferred to a fresh ribonuclease-free tube. RNA samples were then processed using the Zymo RNA clean & concentrator -5 kit (Zymo, R1013), using their RNA clean-up from aqueous phase after TRIzol/chloroform extraction protocol plus on column deoxyribonuclease I treatment. RNA amount was measured using a nanodrop, and integrity was validated through on an Agilent 2100 Bioanalyzer using an RNA nanochip. Samples were sent to Admera Health and sequenced using TruSeq stranded kit.

RNA-seq analysis

Raw paired-end fastqs were processed with TrimGalore (v.0.6.6) (https://github.com/FelixKrueger/TrimGalore) with default settings to remove Illumina adapters and mapped using STAR 2.7.3a (*101*) to the *Drosophila melanogaster* genome annotation dm6. Unmapped and improperly paired reads were filtered out of aligned bam files. Reads per gene in the FlyBase release 2019_05 were computed using an R script using GenomicRanges (v.1.44.0) (*102*) summarizeOverlaps that counts the number of reads overlapping with the exons of each gene in the default "union" mode. Differential expression analysis was performed using DESeq2 (v.1.32.0) (*103*), with count files produced by summarizeOverlaps as input. Principal components analysis (PCA) plots were made using the plotPCA function in DESeq2, with variance stabilized counts as the input. MA plots were constructed from the adjusted *P* values and baseMean values output from DESeq2, and volcano plots were constructed from adjusted *P* values and fold changes reported by DESeq2. Normalized counts produced by DESeq2 were used to show expression levels. Differentially expressed genes were considered to be any gene with an adjusted *P* values of <0.05.

GO and pathway analysis

GO analysis for differentially expressed genes was conducted using FlyMine (v.53) (*104*). The test correction was set to Holm-Bonferroni with a maximum *P* value of 0.05. Kyoto Encyclopedia of Genes and Genomes (KEGG) pathway analysis was done using the "enrichKEGG" function from ClusterProfiler (v.4.0.5) package in R (*105*). A list of all genes with detectable expression was used as background for both GO and pathway analysis (see data S3).

RNAi-based screen of hits from RNA-seq

To understand the mechanisms through which *Atx2* suppresses the TDP-43 sleep phenotype, we focused on genes that were significantly up-regulated with TDP-43 expression and down-regulated with *Atx2* knockdown. We selected RNAi lines available from the Bloomington *Drosophila* Stock Center Transgenic RNAi Project (TRiP) library in a VALIUM20 or greater background. Virgins collected from the *Da*GS>UAS-*TDP-43*^{52S} fly stock were crossed to males of RNAi fly stocks we selected. For controls, we used *Da*GS>UAS-*TDP-43*^{52S} × *UAS-Luciferase* TRiP library control line (BDSC #35788). Male flies were collected, aged, and loaded into RU486 DAM tubes, and sleep assays were performed as described. Total sleep was compared between RNAi lines and control lines to identify genes of interest.

Enzyme-linked immunosorbent assays glucose/glycogen

Glycogen-Glo Assay kit (Promega, CS1823B01) was used to measure glycogen plus glucose levels from *Drosophila* brains using kit protocol. Kit protocol was followed for the assay; briefly, brains were dissected in phosphate-buffered saline and placed in 96-well plates; and luminescence was recorded using CLARIOstar Plus microplate reader.

Western blotting

Brain or head samples were homogenized in sample buffer of 1× Laemmli sample Buffer (Bio-Rad, 1610737), 50 μl β-mercaptoethanol (Sigma-Aldrich, M6250), 1× protease inhibitor (Roche, 11836170001), and 1 mM phenylmethylsulfonyl fluoride (Sigma-Aldrich, P7626). Five microliters of sample buffer is added per brain, 7.5 μl is added per head, and 40 μl is added per whole fly. Samples are boiled at 98°C for 3 min and then centrifuged at 1500 rpm for 3 min at room temperature. Sample was loaded onto 15-well 1.0-mm 4 to 12% bis-tris NuPAGE gels (Thermo Fisher Scientific, WG1401) with prestained protein ladder (Thermo Fisher Scientific, 22619). One brain, one head, or 8% of whole fly tissue is loaded on each lane per experiment. Gel electrophoresis was performed using Xcell Surelock Mini-Cell Electrophoresis System at 140 V and transferred overnight onto a nitrocellulose membrane of 0.45 μM (Bio-Rad, 1620115), using a Bio-Rad mini transblot cell at 90 A for 16 hours. Membranes were stained in Ponceau S (Sigma-Aldrich, P7170-1L), washed in deionized water, and imaged with Amersham Imager 600. Ponceau S was washed off 3× for 5 min in tris-buffered saline with 0.1% Tween 20 (TBST). Membrane was blocked in 5% nonfat dry milk (LabScientific, M08410) in TBST for 1 hour and incubated with primary antibodies with blocking buffer overnight at 4°C. After washing 3× for 5 min in TBST, membranes were incubated with horseradish peroxidase–conjugated secondary antibodies at 1:5000 for 1 hour at room temperature in blocking solution. Membranes were washed 3× for 5 min in TBST, and the signal was develop days using ECL prime (Cytivia, RPN2232) and detected using an Amersham Imager 600. Primary antibodies used the following: antitubulin (1:5000; Developmental Studies Hybridoma Bank, #AA4.3; Lot.5/31/18 to 44 μg/ml) and anti–TDP-43 (1:5000; ProteinTech, #10782-2-AP). Secondary antibodies used the following: goat anti-mouse (1:5000; Jackson lmmunoResearch, #115-035-146, Lot.153978) and goat anti-rabbit (1:5000: Jackson lmmunoResearch, #111-035-144, Lot.138306).

Statistical analysis and data reproducibility

Statistical tests used were performed on GraphPad Prism (v.8 and v.9) and are indicated in the figure legend. *P* values of <0.05 were considered significant. Unpaired two-tailed *t* tests were used when comparing two groups; one-way analysis of variance (ANOVA) was

used when comparing multiple groups, followed by Tukey's posttest when each group was compared against every other group, Sidak's posttest when predefined groups were compared to each other, or Dunnett's test when comparing to a defined control sample. Two-way ANOVA was used when there were two factors in the analysis. One-sided hypergeometric test was used to compare Venn diagram overlaps. Each experiment was generated from a minimum of three independent biological replicates. Samples were allocated on the basis of genotype or experimental manipulation and statistics performed on aggregated data.

Supplementary Materials

This PDF file includes:
Table S1
Figs. S1 to S6
Legends for data S1 to S4

Other Supplementary Material for this manuscript includes the following:
Data S1 to S4

REFERENCES AND NOTES

1. C. Reitz, C. Brayne, R. Mayeux, Epidemiology of Alzheimer disease. *Nat. Rev. Neurol.* **7**, 137–152 (2011).
2. A. Ascherio, M. A. Schwarzschild, The epidemiology of Parkinson's disease: Risk factors and prevention. *Lancet Neurol.* **15**, 1257–1272 (2016).
3. D. V. Petrovsky, M. V. McPhillips, J. Li, A. Brody, L. Caffeé, N. A. Hodgson, Sleep disruption and quality of life in persons with dementia: A state-of-the-art review. *Geriatr. Nurs.* **39**, 640–645 (2018).
4. S. M. McCurry, R. G. Logsdon, L. Teri, L. E. Gibbons, W. A. Kukull, J. D. Bowen, W. C. McCormick, E. B. Larson, Characteristics of sleep disturbance in community-dwelling Alzheimer's disease patients. *J. Geriatr. Psychiatry Neurol.* **12**, 53–59 (1999).
5. J.-E. Kang, M. M. Lim, R. J. Bateman, J. J. Lee, L. P. Smyth, J. R. Cirrito, N. Fujiki, S. Nishino, D. M. Holtzman, Amyloid-beta dynamics are regulated by orexin and the sleep-wake cycle. *Science* **326**, 1005–1007 (2009).
6. J. H. Roh, Y. Huang, A. W. Bero, T. Kasten, F. R. Stewart, R. J. Bateman, D. M. Holtzman, Disruption of the sleep-wake cycle and diurnal fluctuation of β-amyloid in mice with Alzheimer's disease pathology. *Sci. Transl. Med.* **4**, 150ra122 (2012).
7. Y.-E. S. Ju, B. P. Lucey, D. M. Holtzman, Sleep and Alzheimer disease pathology—A bidirectional relationship. *Nat. Rev. Neurol.* **10**, 115–119 (2014).
8. J. K. Holth, S. K. Fritschi, C. Wang, N. P. Pedersen, J. R. Cirrito, T. E. Mahan, M. B. Finn, M. Manis, J. C. Geerling, P. M. Fuller, B. P. Lucey, D. M. Holtzman, The sleep-wake cycle regulates brain interstitial fluid tau in mice and CSF tau in humans. *Science* **363**, 880–884 (2019).
9. C. Wang, D. M. Holtzman, Bidirectional relationship between sleep and Alzheimer's disease: Role of amyloid, tau, and other factors. *Neuropsychopharmacology* **45**, 104–120 (2020).
10. E. S. Musiek, D. D. Xiong, D. M. Holtzman, Sleep, circadian rhythms, and the pathogenesis of Alzheimer disease. *Exp. Mol. Med.* **47**, e148–e148 (2015).
11. J.-F. Gagnon, M. Vendette, R. B. Postuma, C. Desjardins, J. Massicotte-Marquez, M. Panisset, J. Montplaisir, Mild cognitive impairment in rapid eye movement sleep behavior disorder and Parkinson's disease. *Ann. Neurol.* **66**, 39–47 (2009).
12. J.-F. Gagnon, R. B. Postuma, S. Joncas, C. Desjardins, V. Latreille, The Montreal cognitive assessment: A screening tool for mild cognitive impairment in REM sleep behavior disorder. *Mov. Disord.* **25**, 936–940 (2010).
13. P. Congiu, G. Milioli, G. Borghero, F. Marrosu, M. L. Fantini, M. Puligheddu, Impairment of autonomic nervous system in amyotrophic lateral sclerosis. *Sleep Med.* **40**, e271 (2017).
14. P. Congiu, S. Mariani, G. Milioli, L. Parrino, L. Tamburrino, G. Borghero, G. Defazio, B. Pereira, M. L. Fantini, M. Puligheddu, Sleep cardiac dysautonomia and EEG oscillations in amyotrophic lateral sclerosis. *Sleep* **42**, zsz164 (2019).
15. S. Panda, M. Gourie-Devi, A. Sharma, Sleep disorders in amyotrophic lateral sclerosis: A questionnaire-based study from India. *Neurol. India* **66**, 700–708 (2018).
16. L. McGurk, A. Berson, N. M. Bonini, *Drosophila* as an in vivo model for human neurodegenerative disease. *Genetics* **201**, 377–402 (2015).
17. J. M. Shulman, M. B. Feany, Genetic modifiers of tauopathy in *Drosophila*. *Genetics* **165**, 1233–1242 (2003).
18. T.-K. Sang, G. R. Jackson, *Drosophila* models of neurodegenerative disease. *Annu. Rev. Pathol.* **2**, 438–446 (2005).
19. J. M. Shulman, S. Imboywa, N. Giagtzoglou, M. P. Powers, Y. Hu, D. Devenport, P. Chipendo, L. B. Chibnik, A. Diamond, N. Perrimon, N. H. Brown, P. L. De Jager, M. B. Feany, Functional screening in *Drosophila* identifies Alzheimer's disease susceptibility genes and implicates tau-mediated mechanisms. *Hum. Mol. Genet.* **23**, 870–877 (2014).
20. P. Fernandez-Funez, M. L. Nino-Rosales, B. de Gouyon, W. C. She, J. M. Luchak, P. Martinez, E. Turiegano, J. Benito, M. Capovilla, P. J. Skinner, A. McCall, I. Canal, H. T. Orr, H. Y. Zoghbi, J. Botas, Identification of genes that modify ataxin-1-induced neurodegeneration. *Nature* **408**, 101–106 (2000).
21. J. Kim, M. de Haro, I. Al-Ramahi, L. L. Garaicoechea, H.-H. Jeong, J. Y. Sonn, B. Tadros, Z. Liu, J. Botas, H. Y. Zoghbi, Evolutionarily conserved regulators of tau identify targets for new therapies. *Neuron* **111**, 824–838.e7 (2023).
22. L. D. Goodman, M. Prudencio, N. J. Kramer, L. F. Martinez-Ramirez, A. R. Srinivasan, M. Lan, M. J. Parisi, Y. Zhu, J. Chew, C. N. Cook, A. Berson, A. D. Gitler, L. Petrucelli, N. M. Bonini, Toxic expanded GGGGCC repeat transcription is mediated by the PAF1 complex in C9orf72-associated FTD. *Nat. Neurosci.* **22**, 863–874 (2019).
23. J. Bilen, N. M. Bonini, Genome-wide screen for modifiers of ataxin-3 neurodegeneration in *Drosophila*. *PLOS Genet.* **3**, 1950–1964 (2007).
24. A. Berson, A. Sartoris, R. Nativio, V. Van Deerlin, J. B. Toledo, S. Porta, S. Liu, C.-Y. Chung, B. A. Garcia, V. M.-Y. Lee, J. Q. Trojanowski, F. B. Johnson, S. L. Berger, N. M. Bonini, TDP-43 promotes neurodegeneration by impairing chromatin remodeling. *Curr. Biol.* **27**, 3579–3590.e6 (2017).
25. B. D. Freibaum, Y. Lu, R. Lopez-Gonzalez, N. C. Kim, S. Almeida, K.-H. Lee, N. Badders, M. Valentine, B. L. Miller, P. C. Wong, L. Petrucelli, H. J. Kim, F.-B. Gao, J. P. Taylor, GGGGCC repeat expansion in C9orf72 compromises nucleocytoplasmic transport. *Nature* **525**, 129–133 (2015).
26. A. C. Keene, W. J. Joiner, Neurodegeneration: Paying it off with sleep. *Curr. Biol.* **25**, R234–R236 (2015).
27. M. Tabuchi, S. R. Lone, S. Liu, Q. Liu, J. Zhang, A. P. Spira, M. N. Wu, Sleep interacts with aβ to modulate intrinsic neuronal excitability. *Curr. Biol.* **25**, 702–712 (2015).
28. L. Chakravarti, E. H. Moscato, M. S. Kayser, Unraveling the neurobiology of sleep and sleep disorders using *Drosophila*. *Curr. Top. Dev. Biol.* **121**, 253–285 (2017).
29. S. Dissel, M. Klose, J. Donlea, L. Cao, D. English, R. Winsky-Sommerer, B. van Swinderen, P. J. Shaw, Enhanced sleep reverses memory deficits and underlying pathology in *Drosophila* models of Alzheimer's disease. *Neurobiol Sleep Circadian Rhythms* **2**, 15–26 (2017).
30. E. Buhl, J. P. Higham, J. J. L. Hodge, Alzheimer's disease-associated tau alters *Drosophila* circadian activity, sleep and clock neuron electrophysiology. *Neurobiol. Dis.* **130**, 104507 (2019).
31. P. S. Estes, S. G. Daniel, A. P. Mccallum, A. V. Boehringer, A. S. Sukhina, R. A. Zwick, D. C. Zarnescu, Motor neurons and glia exhibit specific individualized responses to TDP-43 expression in a *Drosophila* model of amyotrophic lateral sclerosis. *Dis. Model. Mech.* **6**, 721–733 (2013).
32. X. Sun, D. Ran, X. Zhao, Y. Huang, S. Long, F. Liang, W. Guo, F. C. Nucifora, H. Gu, X. Lu, L. Chen, J. Zeng, C. A. Ross, Z. Pei, Melatonin attenuates hLRRK2-induced sleep disturbances and synaptic dysfunction in a *Drosophila* model of Parkinson's disease. *Mol. Med. Rep.* **13**, 3936–3944 (2016).
33. K. Ito, H. Kawasaki, T. Suzuki, T. Takahara, N. Ishida, Effects of kamikihito and unkei-to on sleep behavior of wild type and Parkinson model in *Drosophila*. *Front. Psych.* **8**, (2017).
34. S. J. Belfer, A. G. Bashaw, M. L. Perlis, M. S. Kayser, A *Drosophila* model of sleep restriction therapy for insomnia. *Mol. Psychiatry* **26**, 492–507 (2021).
35. M. Neumann, D. M. Sampathu, L. K. Kwong, A. C. Truax, M. C. Micsenyi, T. T. Chou, J. Bruce, T. Schuck, M. Grossman, C. M. Clark, L. F. McCluskey, B. L. Miller, E. Masliah, I. R. Mackenzie, H. Feldman, W. Feiden, H. A. Kretzschmar, J. Q. Trojanowski, V. M.-Y. Lee, Ubiquitinated TDP-43 in frontotemporal lobar degeneration and amyotrophic lateral sclerosis. *Science* **314**, 130–133 (2006).
36. C. Lagier-Tourenne, D. W. Cleveland, Rethinking ALS: The FUS about TDP-43. *Cell* **136**, 1001–1004 (2009).
37. G. S. Pesiridis, V. M.-Y. Lee, J. Q. Trojanowski, Mutations in TDP-43 link glycine-rich domain functions to amyotrophic lateral sclerosis. *Hum. Mol. Genet.* **18**, R156–R162 (2009).
38. K. A. Josephs, D. W. Dickson, N. Tosakulwong, S. D. Weigand, M. E. Murray, L. Petrucelli, A. M. Liesinger, M. L. Senjem, A. J. Spychalla, D. S. Knopman, J. E. Parisi, R. C. Petersen, C. R. Jack, J. L. Whitwell, Rates of hippocampal atrophy and presence of post-mortem TDP-43 in patients with Alzheimer's disease: A longitudinal retrospective study. *Lancet Neurol.* **16**, 917–924 (2017).
39. K. E. McAleese, L. Walker, D. Erskine, A. J. Thomas, I. G. McKeith, J. Attems, TDP-43 pathology in Alzheimer's disease, dementia with Lewy bodies and ageing. *Brain Pathol.* **27**, 472–479 (2017).
40. K. A. Josephs, M. E. Murray, J. L. Whitwell, N. Tosakulwong, S. D. Weigand, L. Petrucelli, A. M. Liesinger, R. C. Petersen, J. E. Parisi, D. W. Dickson, Updated TDP-43 in Alzheimer's disease staging scheme. *Acta Neuropathol.* **131**, 571–585 (2016).

41. B. D. James, R. S. Wilson, P. A. Boyle, J. Q. Trojanowski, D. A. Bennett, J. A. Schneider, TDP-43 stage, mixed pathologies, and clinical Alzheimer's-type dementia. *Brain* **139**, 2983–2993 (2016).
42. K. A. Josephs, J. L. Whitwell, S. D. Weigand, M. E. Murray, N. Tosakulwong, A. M. Liesinger, L. Petrucelli, M. L. Senjem, D. S. Knopman, B. F. Boeve, R. J. Ivnik, G. E. Smith, C. R. Jack, J. E. Parisi, R. C. Petersen, D. W. Dickson, TDP-43 is a key player in the clinical features associated with Alzheimer's disease. *Acta Neuropathol.* **127**, 811–824 (2014).
43. T. F. Gendron, L. Petrucelli, Rodent models of TDP-43 proteinopathy: Investigating the mechanisms of TDP-43-mediated neurodegeneration. *J. Mol. Neurosci.* **45**, 486–499 (2011).
44. E. B. Lee, V. M.-Y. Lee, J. Q. Trojanowski, Gains or losses: Molecular mechanisms of TDP43-mediated neurodegeneration. *Nat. Rev. Neurosci.* **13**, 38–50 (2011).
45. C. Lagier-Tourenne, D. W. Cleveland, Rethinking ALS: The FUS about TDP-43. *Cell* **136**, 1001–1004 (2009).
46. H. J. Kim, A. R. Raphael, E. S. Ladow, L. Mcgurk, R. A. Weber, J. Q. Trojanowski, V. M. Y. Lee, S. Finkbeiner, A. D. Gitler, N. M. Bonini, Therapeutic modulation of eIF2α phosphorylation rescues TDP-43 toxicity in amyotrophic lateral sclerosis disease models. *Nat. Genet.* **46**, 152–160 (2014).
47. L. McGurk, E. Gomes, L. Guo, J. Mojsilovic-Petrovic, V. Tran, R. G. Kalb, J. Shorter, N. M. Bonini, Poly(ADP-ribose) prevents pathological phase separation of tdp-43 by promoting liquid demixing and stress granule localization. *Mol. Cell* **71**, 703–717.e9 (2018).
48. Y. M. Ayala, P. Zago, A. D'Ambrogio, Y.-F. Xu, L. Petrucelli, E. Buratti, F. E. Baralle, Structural determinants of the cellular localization and shuttling of TDP-43. *J. Cell Sci.* **121**, 3778–3785 (2008).
49. B. I. Nilaver, H. F. Urbanski, Mechanisms underlying TDP-43 pathology and neurodegeneration: An updated mini-review. *Front. Aging Neurosci.* **15**, 1142617 (2023).
50. A. Joardar, E. Manzo, D. C. Zarnescu, Metabolic dysregulation in amyotrophic lateral sclerosis: Challenges and opportunities. *Curr Genet Med Rep* **5**, 108–114 (2017).
51. H. Blasco, D. Lanznaster, C. Veyrat-Durebex, R. Hergesheimer, P. Vourch, F. Maillot, C. R. Andres, P.-F. Pradat, P. Corcia, Understanding and managing metabolic dysfunction in amyotrophic lateral sclerosis. *Expert Rev. Neurother.* **20**, 907–919 (2020).
52. J. C. Dodge, C. M. Treleaven, J. A. Fidler, T. J. Tamsett, C. Bao, M. Searles, T. V. Taksir, K. Misra, R. L. Sidman, S. H. Cheng, L. S. Shihabuddin, Metabolic signatures of amyotrophic lateral sclerosis reveal insights into disease pathogenesis. *Proc. Natl. Acad. Sci. U.S.A.* **110**, 10812–10817 (2013).
53. C. Li, Q. Wei, X. Gu, Y. Chen, X. Chen, B. Cao, R. Ou, H. Shang, Decreased glycogenolysis by mir-338-3p promotes regional glycogen accumulation within the spinal cord of amyotrophic lateral sclerosis mice. *Front Mol. Neurosci.* **12**, 114 (2019).
54. S. Krupp, I. Hubbard, O. Tam, G. M. Hammell, J. Dubnau, TDP-43 pathology in *Drosophila* induces glial-cell type specific toxicity that can be ameliorated by knock-down of SF2/SRSF1. *PLOS Genet.* **19**, e1010973 (2023).
55. L. Krug, N. Chatterjee, R. Borges-Monroy, S. Hearn, W.-W. Liao, K. Morrill, L. Prazak, N. Rozhkov, D. Theodorou, M. Hammell, J. Dubnau, Retrotransposon activation contributes to neurodegeneration in a *Drosophila* TDP-43 model of ALS. *PLOS Genet.* **13**, e1006635 (2017).
56. C.-Y. Chung, A. Berson, J. R. Kennerdell, A. Sartoris, T. Unger, S. Porta, H.-J. Kim, E. R. Smith, A. Shilatifard, V. Van Deerlin, V. M.-Y. Lee, A. Chen-Plotkin, N. M. Bonini, Aberrant activation of non-coding RNA targets of transcriptional elongation complexes contributes to TDP-43 toxicity. *Nat. Commun.* **9**, 4406 (2018).
57. L. François-Moutal, D. D. Scott, A. J. Ambrose, C. J. Zerio, M. Rodriguez-Sanchez, K. Dissanayake, D. G. May, J. M. Carlson, E. Barbieri, A. Moutal, K. J. Roux, J. Shorter, R. Khanna, S. J. Barmada, L. McGurk, M. Khanna, Heat shock protein Grp78/BiP/HspA5 binds directly to TDP-43 and mitigates toxicity associated with disease pathology. *Sci. Rep.* **12**, 8140 (2022).
58. A. C. Elden, H. J. Kim, M. P. Hart, A. S. Chen-Plotkin, B. S. Johnson, X. Fang, M. Armakola, F. Geser, R. Greene, M. M. Lu, A. Padmanabhan, D. Clay-Falcone, L. McCluskey, L. Elman, D. Juhr, P. J. Gruber, U. Rüb, G. Auburger, J. Q. Trojanowski, V. M. Y. Lee, V. M. Van Deerlin, N. M. Bonini, A. D. Gitler, Ataxin-2 intermediate-length polyglutamine expansions are associated with increased risk for ALS. *Nature* **466**, 1069–1075 (2010).
59. L. A. Becker, B. Huang, G. Bieri, R. Ma, D. A. Knowles, P. Jafar-Nejad, J. Messing, H. J. Kim, A. Soriano, G. Auburger, S. M. Pulst, J. P. Taylor, F. Rigo, A. D. Gitler, Therapeutic reduction of ataxin-2 extends lifespan and reduces pathology in TDP-43 mice. *Nature* **544**, 367–371 (2017).
60. S. M. J. McBride, C. H. Choi, B. P. Schoenfeld, A. J. Bell, D. A. Liebelt, D. Ferreiro, R. J. Choi, P. Hinchey, M. Kollaros, A. M. Terlizzi, N. J. Ferrick, E. Koenigsberg, R. L. Rudominer, A. Sumida, S. Chiorean, K. K. Siwicki, H. T. Nguyen, M. E. Fortini, T. V. McDonald, T. A. Jongens, Pharmacological and genetic reversal of age-dependent cognitive deficits attributable to decreased presenilin function. *J. Neurosci.* **30**, 9510–9522 (2010).
61. S. D. Mhatre, S. J. Michelson, J. Gomes, L. P. Tabb, A. J. Saunders, D. R. Marenda, Development and characterization of an aged onset model of Alzheimer's disease in *Drosophila melanogaster*. *Exp. Neurol.* **261**, 772–781 (2014).
62. C. W. Wittmann, M. F. Wszolek, J. M. Shulman, P. M. Salvaterra, J. Lewis, M. Hutton, M. B. Feany, Tauopathy in *Drosophila*: Neurodegeneration without neurofibrillary tangles. *Science* **293**, 711–714 (2001).
63. M. Tabuchi, S. R. Lone, S. Liu, Q. Liu, J. Zhang, A. P. Spira, M. N. Wu, Sleep interacts with aβ to modulate intrinsic neuronal excitability. *Curr. Biol.* **25**, 702–712 (2015).
64. K. Iijima, H.-C. Chiang, S. A. Hearn, I. Hakker, A. Gatt, C. Shenton, L. Granger, A. Leung, K. Iijima-Ando, Y. Zhong, Aβ42 mutants with different aggregation profiles induce distinct pathologies in *Drosophila*. *PLOS One* **3**, e1703 (2008).
65. S. D. Mhatre, S. J. Michelson, J. Gomes, L. P. Tabb, A. J. Saunders, D. R. Marenda, Development and characterization of an aged onset model of Alzheimer's disease in *Drosophila* melanogaster. *Exp. Neurol.* **261**, 772–781 (2014).
66. N. J. Kramer, Y. Carlomagno, Y.-J. Zhang, S. Almeida, C. N. Cook, T. F. Gendron, M. Prudencio, M. Van Blitterswijk, V. Belzil, J. Couthouis, J. W. Paul, L. D. Goodman, L. Daughrity, J. Chew, A. Garrett, L. Pregent, K. Jansen-West, L. J. Tabassian, R. Rademakers, K. Boylan, N. R. Graff-Radford, K. A. Josephs, J. E. Parisi, D. S. Knopman, R. C. Petersen, B. F. Boeve, N. Deng, Y. Feng, T.-H. Cheng, D. W. Dickson, S. N. Cohen, N. M. Bonini, C. D. Link, F.-B. Gao, L. Petrucelli, A. D. Gitler, Spt4 selectively regulates the expression of C9orf72 sense and antisense mutant transcripts. *Science* **353**, 708–712 (2016).
67. P. K. Auluck, H. Y. E. Chan, J. Q. Trojanowski, V. M. Y. Lee, N. M. Bonini, Chaperone suppression of α-synuclein toxicity in a *Drosophila* model for Parkinson's disease. *Science* **295**, 865–868 (2002).
68. M. B. Feany, W. W. Bender, A *Drosophila* model of Parkinson's disease. *Nature* **404**, 394–398 (2000).
69. J. Kang, S. Shin, N. Perrimon, J. Shen, An evolutionarily conserved role of presenilin in neuronal protection in the aging *Drosophila* brain. *Genetics* **206**, 1479–1493 (2017).
70. H.-J. Kim, A. R. Raphael, E. S. LaDow, L. McGurk, R. Weber, J. Q. Trojanowski, V. M.-Y. Lee, S. Finkbeiner, A. D. Gitler, N. M. Bonini, Therapeutic modulation of eIF2α-phosphorylation rescues TDP-43 toxicity in amyotrophic lateral sclerosis disease models. *Nat. Genet.* **46**, 152–160 (2014).
71. M. E. Yurgel, P. Masek, J. DiAngelo, A. C. Keene, Genetic dissection of sleep-metabolism interactions in the fruit fly. *J. Comp. Physiol. A Neuroethol. Sens. Neural Behav. Physiol.* **201**, 869–877 (2015).
72. T. W. Tefera, K. Borges, Metabolic dysfunctions in amyotrophic lateral sclerosis pathogenesis and potential metabolic treatments. *Front. Neurosci.* **10**, 611 (2016).
73. L. N. Bell, J. M. Kilkus, J. N. Booth, L. E. Bromley, J. G. Imperial, P. D. Penev, Effects of sleep restriction on the human plasma metabolome. *Physiol. Behav.* **122**, 25–31 (2013).
74. T. Lerskiatiphanich, J. Marallag, J. D. Lee, Glucose metabolism in amyotrophic lateral sclerosis: It is bitter-sweet. *Neural Regen. Res.* **17**, 1975–1977 (2022).
75. J. L. Bedont, H. Toda, M. Shi, C. H. Park, C. Quake, C. Stein, A. Kolesnik, A. Sehgal, Short and long sleeping mutants reveal links between sleep and macroautophagy. *eLife* **10**, e64140 (2021).
76. K. D. Finley, P. T. Edeen, R. C. Cumming, M. D. Mardahl-Dumesnil, B. J. Taylor, M. H. Rodriguez, C. E. Hwang, M. Benedetti, M. McKeown, Blue cheese mutations define a novel, conserved gene involved in progressive neural degeneration. *J. Neurosci.* **23**, 1254–1264 (2003).
77. A. Simonsen, R. C. Cumming, K. D. Finley, Linking lysosomal trafficking defects with changes in aging and stress response in *Drosophila*. *Autophagy* **3**, 499–501 (2007).
78. J. W. Lee, S. Park, Y. Takahashi, H.-G. Wang, The association of AMPK with ULK1 regulates autophagy. *PLOS One* **5**, e15394 (2010).
79. J. Zirin, J. Nieuwenhuis, N. Perrimon, Role of autophagy in glycogen breakdown and its relevance to chloroquine myopathy. *PLoS Biol.* **11**, e1001708 (2013).
80. A. Berson, A. Sartoris, R. Nativio, V. Van Deerlin, J. B. Toledo, S. Porta, S. Liu, C.-Y. Chung, B. A. Garcia, V. M.-Y. Lee, J. Q. Trojanowski, F. B. Johnson, S. L. Berger, N. M. Bonini, TDP-43 promotes neurodegeneration by impairing chromatin remodeling. *Curr. Biol.* **27**, 3579–3590.e6 (2017).
81. A. C. Keene, E. R. Duboué, D. M. McDonald, M. Dus, G. S. B. Suh, S. Waddell, J. Blau, Clock and cycle limit starvation-induced sleep loss in *Drosophila*. *Curr. Biol.* **20**, 1209–1215 (2010).
82. C.-W. Cheng, M.-J. Lin, C.-K. J. Shen, Rapamycin alleviates pathogenesis of a new *Drosophila* model of ALS-TDP. *J. Neurogenet.* **29**, 59–68 (2015).
83. F. Parisi, S. Riccardo, M. Daniel, M. Saqcena, N. Kundu, A. Pession, D. Grifoni, H. Stocker, E. Tabak, P. Bellosta, *Drosophila* insulin and target of rapamycin (TOR) pathways regulate GSK3 beta activity to control Myc stability and determine Myc expression in vivo. *BMC Biol.* **9**, 65 (2011).
84. I. Bjedov, J. M. Toivonen, F. Kerr, C. Slack, J. Jacobson, A. Foley, L. Partridge, Mechanisms of life span extension by rapamycin in the fruit fly *Drosophila* melanogaster. *Cell Metab.* **11**, 35–46 (2010).
85. S. H. Ou, F. Wu, D. Harrich, L. F. García-Martínez, R. B. Gaynor, Cloning and characterization of a novel cellular protein, TDP-43, that binds to human immunodeficiency virus type 1 TAR DNA sequence motifs. *J. Virol.* **69**, 3584–3596 (1995).
86. K. Weskamp, S. J. Barmada, TDP43 and RNA instability in amyotrophic lateral sclerosis. *Brain Res.* **1693**, 67–74 (2018).

87. M. Neumann, Molecular neuropathology of TDP-43 proteinopathies. *Int. J. Mol. Sci.* **10**, 232–246 (2009).
88. M. Boentert, Sleep disturbances in patients with amyotrophic lateral sclerosis: Current perspectives. *Nat Sci Sleep*, 97–111 (2019).
89. Y. Zhuang, Z. Li, S. Xiong, C. Sun, B. Li, S. A. Wu, J. Lyu, X. Shi, L. Yang, Y. Chen, Z. Bao, X. Li, C. Sun, Y. Chen, H. Deng, T. Li, Q. Wu, L. Qi, Y. Huang, X. Yang, Y. Lin, Circadian clocks are modulated by compartmentalized oscillating translation. *Cell* **186**, 3245–3260.e23 (2023).
90. Y. Zhang, J. Ling, C. Yuan, R. Dubruille, P. Emery, A role for *Drosophila* ATX2 in activation of PER translation and circadian behavior. *Science* **340**, 879–882 (2013).
91. C. Lim, R. Allada, ATAXIN-2 activates PERIOD translation to sustain circadian rhythms in *Drosophila*. *Science* **340**, 875–879 (2013).
92. S. B. Lee, S. Kim, J. Lee, J. Park, G. Lee, Y. Kim, J.-M. Kim, J. Chung, ATG1, an autophagy regulator, inhibits cell growth by negatively regulating S6 kinase. *EMBO Rep.* **8**, 360–365 (2007).
93. T. W. Tefera, F. J. Steyn, S. T. Ngo, K. Borges, CNS glucose metabolism in amyotrophic lateral sclerosis: A therapeutic target? *Cell Biosci.* **11**, 14 (2021).
94. D. Meierhofer, M. Halbach, N. E. Şen, S. Gispert, G. Auburger, Ataxin-2 (Atxn2)-knock-out mice show branched chain amino acids and fatty acids pathway alterations. *Mol. Cell. Proteomics* **15**, 1728–1739 (2016).
95. I. Lastres-Becker, U. Rüb, G. Auburger, Spinocerebellar ataxia 2 (SCA2). *Cerebellum* **7**, 115–124 (2008).
96. I. Lastres-Becker, S. Brodesser, D. Lütjohann, M. Azizov, J. Buchmann, E. Hintermann, K. Sandhoff, A. Schürmann, J. Nowock, G. Auburger, Insulin receptor and lipid metabolism pathology in ataxin-2 knock-out mice. *Hum. Mol. Genet.* **17**, 1465–1481 (2008).
97. M. C. B. Vianna, D. C. Poleto, P. F. Gomes, V. Valente, M. L. Paçó-Larson, *Drosophila* ataxin-2 gene encodes two differentially expressed isoforms and its function in larval fat body is crucial for development of peripheral tissues. *FEBS Open Bio.* **6**, 1040–1053 (2016).
98. I. Lastres-Becker, D. Nonis, F. Eich, M. Klinkenberg, M. Gorospe, P. Kötter, F. A. C. Klein, N. Kedersha, G. Auburger, Mammalian ataxin-2 modulates translation control at the pre-initiation complex via PI3K/mTOR and is induced by starvation. *Biochim Biophys Acta.* **1862**, 1558–1569 (2016).
99. G. F. Gilestro, Video tracking and analysis of sleep in *Drosophila melanogaster*. *Nat. Protoc.* **7**, 995–1007 (2012).
100. Q. Geissmann, L. G. Rodriguez, E. J. Beckwith, G. F. Gilestro, Rethomics: An R framework to analyse high-throughput behavioural data. *PLOS One* **14**, e0209331 (2019).
101. A. Dobin, C. A. Davis, F. Schlesinger, J. Drenkow, C. Zaleski, S. Jha, P. Batut, M. Chaisson, T. R. Gingeras, STAR: Ultrafast universal RNA-seq aligner. *Bioinformatics* **29**, 15–21 (2013).
102. M. Lawrence, W. Huber, H. Pagès, P. Aboyoun, M. Carlson, R. Gentleman, M. T. Morgan, V. J. Carey, Software for computing and annotating genomic ranges. *PLOS Comput. Biol.* **9**, e1003118 (2013).
103. M. I. Love, W. Huber, S. Anders, Moderated estimation of fold change and dispersion for RNA-seq data with DESeq2. *Genome Biol.* **15**, 550 (2014).
104. R. N. Smith, J. Aleksic, D. Butano, A. Carr, S. Contrino, F. Hu, M. Lyne, R. Lyne, A. Kalderimis, K. Rutherford, R. Stepan, J. Sullivan, M. Wakeling, X. Watkins, G. Micklem, InterMine: A flexible data warehouse system for the integration and analysis of heterogeneous biological data. *Bioinformatics* **28**, 3163–3165 (2012).
105. G. Yu, L.-G. Wang, Y. Han, Q.-Y. He, ClusterProfiler: An R package for comparing biological themes among gene clusters. *OMICS* **16**, 284–287 (2012).

Acknowledgments: We thank members of the Kayser laboratory and Bonini laboratory. We thank L. McGurk for sharing *Atx2* RNAi lines and J. Bedont for helpful input on the study. We thank the *Drosophila* Genomics Resource Center (NIH grant 2P40OD010949) and the Bloomington *Drosophila* Stock Center (NIH P40OD018537) for fly lines. We thank the TRiP at Harvard Medical School (NIH/NIGMS R01-GM084947) for RNAi fly stocks. Figure 9 was made using http://BioRender.com. **Funding:** This work was supported by NIH grants F31-AG063470 (to A.E.P.), F32-NS117785 and T32-MH014654 (to J.D.), F30-AG058409 and T32-HL07953 (to S.J.B.), R56-AG071777 and R01-AG071777 (to M.S.K. and N.M.B.), a pilot grant (to M.S.K.) from the University of Pennsylvania Alzheimer's Disease Core Center (P30-AG010124), and Burroughs Wellcome Career Award for Medical Scientists (to M.S.K.). **Author contributions:** A.E.P. conceived, designed, performed the experiments, statistical analysis, bioinformatic analysis, and analyzed the data. J.D. conceived, designed, performed the sleep experiments, and analyzed the data. S.J.B conceived, designed, performed the sleep experiments, and analyzed the data. A.R., O.S., K.P., and J.L. performed the experiments. M.S.K. and N.M.B. conceived, designed the experiments, analyzed the data, and supervised the research. A.E.P., N.M.B., and M.S.K. wrote the manuscript, with feedback from all authors. **Competing interests:** The authors declare that they have no competing interests. **Data and materials availability:** All data needed to evaluate the conclusions in the paper are present in the paper and/or the Supplementary Materials. The raw sequencing data generated in this study have been deposited in the Gene Expression Omnibus under accession GSE234468 (www.ncbi.nlm.nih.gov/geo/query/acc.cgi?acc=GSE234468).

Submitted 29 June 2023
Accepted 12 December 2023
Published 10 January 2024
10.1126/sciadv.adj4457